NATIONAL ADVISORY COMMITTEE FOR AERONAUTICS

TECHNICAL NOTE 3898

WIND-TUNNEL INVESTIGATION OF AN EXTERNAL-FLOW JET-AUGMENTED SLOTTED FLAP SUITABLE FOR APPLICATION TO AIRPLANES WITH POD-MOUNTED JET ENGINES

By John P. Campbell and Joseph L. Johnson, Jr.

Langley Aeronautical Laboratory
Langley Field, Va.

Washington
December 1956

NATIONAL ADVISORY COMMITTEE FOR AERONAUTICS

TECHNICAL NOTE 3898

WIND-TUNNEL INVESTIGATION OF AN EXTERNAL-FLOW JET-AUGMENTED SLOTTED FLAP SUITABLE FOR APPLICATION TO AIRPLANES WITH POD-MOUNTED JET ENGINES

By John P. Campbell and Joseph L. Johnson, Jr.

SUMMARY

A wind-tunnel investigation has been carried out to determine the characteristics of an external-flow jet-augmented slotted flap which appears suitable for application to airplanes with pod-mounted jet engines. The investigation included tests of an unswept wing and of a model of a swept-wing jet transport or bomber. Compressed air jets exhausting from nozzles attached to the lower surface of the wings were used to simulate the jets from pod-mounted jet engines.

The external-flow jet-augmented flap produced values of circulation lift large enough to warrant serious consideration of its use for increasing the maximum lift coefficients of airplanes with pod-mounted jet engines. The results indicated that static longitudinal stability and trim up to a lift coefficient of at least 6 could be achieved with a jet transport or bomber airplane equipped with a jet-augmented flap and having a horizontal-tail area equal to 25 percent of the wing area. In order to achieve this result, it was necessary to locate the horizontal tail in a position well above the chord plane of the wing and to incorporate both variable tail incidence and an elevator. The results indicated that an external-flow jet-augmented flap applied to existing jet transport and bomber airplanes with pod-mounted engines would produce lift coefficients of about 3 for take-off (thrust-weight ratio of 0.25) and lift coefficients of about 5 for landing (thrust-weight ratio of 0.40). These lift coefficients would provide substantial reductions in take-off and landing speeds and distances.

INTRODUCTION

Recent investigations in Great Britain (refs. 1 and 2), in France (ref. 3), and in this country (refs. 4 and 5) have indicated promise for the jet flap, a scheme in which all the propulsive jet is deflected

downward through a narrow full-span nozzle at the trailing edge of the wing to produce very high lift coefficients. On the basis of the promising results obtained in these investigations, a study was recently undertaken by the Langley Free Flight Tunnel Section of the National Advisory Committee for Aeronautics to establish the configuration of a free-flying model incorporating a jet flap for an investigation of the stability and control at the high lift coefficients that can be obtained with such flap arrangements.

At an early stage in this preliminary design study, a new type of jet flap which might be applied more easily to jet transport and bomber airplanes with pod-mounted engines was conceived. In this arrangement, called an external-flow jet-augmented slotted flap (in contrast to the internal-flow jet flap), the jet from a pod-mounted engine is directed toward the base of a slotted flap which deflects the jet downward in the form of a flattened jet sheet. In one form of this arrangement, a retractable deflector at the engine tail pipe can be used to deflect the jet toward the flap and at the same time produce some flattening of the jet. For cruising flight, both the deflector and the flap would be retracted so that the airplane would be a conventional pod-engine configuration. For take-off, the deflector and flap would not be extended until the airplane has accelerated almost to the take-off speed.

One of the obvious problems which will be encountered with any jet-flap or jet-augmented-flap arrangement which utilizes hot exhaust gases of jet engines is that of the high temperatures. With this particular external-flow arrangement, high temperatures and high localized loads will be experienced over the rear portion of the wing and over the flaps. It is believed that these high temperatures and structural problems can be solved by the use of existing materials and fabrication techniques.

Since the inherent simplicity of the external-flow jet-augmented flap made it appear promising, a brief force-test investigation was undertaken to determine whether its performance would closely approach that of the internal-flow type of jet flap reported in references 1 to 5. The investigation included force tests to determine the lift, drag, and pitching moments of an aspect-ratio-6 unswept wing with simple compressed-air nozzles attached to the lower surface to represent pod-mounted jet engines. Tests were made with both plain and slotted flaps at various deflections and the results obtained were compared with data from reference 5.

Also included in this investigation were tests of a jet bomber or transport configuration having a 30° sweptback wing of aspect ratio 6.6 and equipped with various arrangements of pod-mounted engines. Tests were made of the swept wing alone, of two wing-fuselage combinations, and of the complete model with several different horizontal-tail arrangements. Some of the data obtained were used to make estimates of

the reductions in take-off and landing speeds that might be achieved by the use of an external-flow jet-augmented flap on jet transport or bomber configurations having pod-mounted engines.

SYMBOLS

Data for the unswept and swept wings are referred to a center of gravity located at 0.25 mean aerodynamic chord and on the chord plane of the wing. The data for the sweptback-wing transport model are referred to a center of gravity located on the reference line of the fuselage and at 0.25 or 0.40 mean aerodynamic chord.

S	wing area, sq ft
$\bar{c}$	mean aerodynamic chord, ft
V	velocity, knots
q	dynamic pressure, $\frac{1}{2}\rho V^2$, lb/sq ft
ρ	air density, slugs/cu ft
W	weight, lb
T	thrust, lb
α	angle of attack, deg
M_Y	pitching moment, ft-lb
C_L	lift coefficient, Lift/qS
C_μ	momentum coefficient based on thrust measured at nozzle, T/qS
C_D	drag coefficient, Drag/qS
C_m	pitching-moment coefficient, $M_Y/qS\bar{c}$
$C_{m_\alpha} = \frac{\partial C_m}{\partial \alpha}$	per deg
$\frac{\partial C_m}{\partial C_L}$	static margin

S_t horizontal-tail area, sq ft

i_t incidence of horizontal tail, deg

δ_f flap deflection, perpendicular to flap hinge line, deg

$C_{L,\Gamma}$ jet circulation lift coefficient, $C_L - (C_L)_{C_\mu=0} - C_\mu \sin(\alpha + \delta_f)$

The subscripts 0.25 and 0.40 denote moment reference location in percent mean aerodynamic chord.

APPARATUS AND MODELS

The investigation was conducted in the Langley full-scale tunnel. All tests were made with a vertical strut-support system and strain-gage balances. The test setup was located in the forward portion of the test section near the lower lip of the entrance cone.

A drawing of the unswept wing tested in this investigation is shown in figure 1 and dimensional characteristics are presented in table I. The aspect ratio of this wing was 6 and the airfoil section was NACA 0012 at the root and tip. The unswept-wing arrangement was a rather crude setup used in the preliminary evaluation of the external-flow jet-augmented flap. Pod-mounted engines were simulated by eight simple nozzles which were spaced equally along the span of the wing, and the air jets were flattened and directed toward the base of the flap by flat-plate deflectors. Cold air jets were used to simulate the jet-engine exhaust. Compressed air was supplied to each nozzle through flexible hoses which were attached externally for the tests made with the unswept wing. The unswept wing was tested with a plain flap and a slotted flap. (See fig. 1.)

The various configurations of the sweptback-wing jet transport or bomber model used in the investigation are shown in figures 2 and 3 and dimensional characteristics are given in table I. The wing of the model had 30° sweep of the quarter chord, an aspect ratio of 6.62, and a taper ratio of 0.367. The airfoil section was NACA 65_1-414 at the root and NACA 65-410 at the tip. Six nacelles were attached to the wing on pylons to simulate pod-mounted engines. These nacelles could be located at various positions over the inboard two-thirds of the span and could be tested in groups of 2, 4, or 6. Compressed air was supplied to each nacelle by flexible hoses passed internally through the fuselage and wing.

A detail drawing of the jet-flap arrangement used on the swept-wing model is shown in figure 4. For take-off and landing, the jets from the pod-mounted engines are spread out into a horizontal sheet by retractable

deflectors and directed toward the base of a slotted flap which then turns the flattened jet sheet downward. Another configuration used on the model was one in which no deflector was used and the tail pipe was tilted to direct the jet toward the bottom surface of the wing near the base of the flap. The full-span slotted flap was hinged on the bottom surface of the wing so that a smooth fairing was obtained between the wing and flap for all flap deflections. With the flap deflected, the upper lip of the slot was alined with the lower surface of the wing.

TESTS

Preliminary tests at an angle of attack of 0° were made to determine the lift, drag, and pitching moments of the unswept wing alone in order to evaluate the external-flow jet-augmented flap arrangement. These tests were made at momentum coefficients up to about 8 for plain and slotted flap configurations.

On the basis of the favorable results obtained with the unswept wing alone, tests were made at an angle of attack of 0° to determine the aerodynamic characteristics of the swept-wing jet transport model. This model was tested in various configurations which included the wing alone with either two or six jets and the wing in combination with a fuselage in both high- and low-wing arrangements.

Longitudinal stability and trim tests were made over an angle-of-attack range from -8° to 12° for the high-wing two-jet configuration. These tests were made for the model with two horizontal tails of different size and for two different locations of the horizontal tail on the vertical tail. For some tests, the horizontal tail was equipped with leading-edge and trailing-edge flaps.

All the tests in this investigation were made at a dynamic pressure of about 1.6 pounds per square foot which corresponds to a velocity of about 21.8 knots and to a Reynolds number range of about 160,000 to 170,000 based on the mean aerodynamic chords of the wings tested.

REDUCTION OF DATA

No wind-tunnel corrections have been applied to the data since the model was relatively small compared with the size of the tunnel test section.

The coefficient C_μ used in this report is defined as T/qS where T is the measured thrust at the nozzle which represents the tail pipe of

a jet engine. This coefficient is approximately equivalent to the momentum coefficient C_μ which has been used in boundary-layer-control investigations and in the jet-flap investigations reported in references 4 and 5. The values of thrust used in establishing this coefficient were obtained from force measurements made during static calibrations of the cruising configuration (flaps and deflectors retracted) and of the landing configuration (flaps and deflectors extended). Comparison of the calibration data for these two conditions indicated that the losses caused by spreading and deflecting the jet were about 20 percent for the 40° and 50° flap deflections, 25 percent for the 60° flap deflection, and 30 percent for the 70° deflection. For cases in which the static calibration was made only in the landing configuration, it was necessary to apply these corrections to the thrust measurements to obtain the thrust at the nozzle in order to establish C_μ.

RESULTS AND DISCUSSION

Unswept Wings

Jet-augmented plain flap.- In the preliminary evaluation of the external-flow jet-augmented flap, tests were first made on an aspect-ratio-6 unswept wing having a 25-percent-chord plain flap (fig. 1). The jets from eight simulated pod-mounted engines located equally along the span were spread out by deflectors and directed toward the base of a plain flap which deflected the jet downward. The results of tests of this arrangement are presented in figure 5. In order to aid in the evaluation of the effectiveness of this arrangement, the vertical component of the thrust leaving the flap, called the reaction lift $C_\mu \sin(\alpha + \delta_f)$, and the lift at $C_\mu = 0$ have also been plotted in figure 5 for the 60° flap deflection. The jet-induced or circulation lift $C_{L,\Gamma}$ can be taken as the difference between the total lift and the sum of the lift at $C_\mu = 0$ and the reaction lift. This procedure for obtaining circulation lift is similar to that presented in reference 4 but, as pointed out in that reference, such a procedure gives values of circulation lift that are actually somewhat smaller than the true values. The data of figure 5 show that the greater part of the total lift in this case was the reaction component $C_\mu \sin(\alpha + \delta_f)$ but that some circulation lift was obtained.

Jet-augmented slotted flap.- In order to determine whether more circulation lift could be obtained if the flattened jet sheet were made to pass through a slot and over the back side of the flap, the aspect-ratio-6 unswept wing was equipped with a slotted flap as shown in figure 1. The data obtained with this arrangement are shown in figure 6. These data indicate that, for the same flap deflection, the circulation lift for the slotted flap was about twice that obtained for the plain flap.

Comparison of jet flaps.- The values of circulation lift for the jet-augmented plain and slotted flap configurations for 60° flap deflection plotted against C_μ are presented in figure 7. For comparison, corresponding data for an internal-flow jet flap taken from figure 4 of reference 5 are also shown in figure 7. These data show that the external-flow jet-augmented flap is not as effective in producing lift as the internal-flow jet flap but, in the slotted-flap arrangement, it produces values of circulation lift that are large enough to warrant its consideration for use on airplanes with pod-mounted engines.

Swept Wings

Effect of sweep.- Data from tests of the swept and unswept wings alone with the external-flow jet-augmented slotted flap are presented in figure 8. The swept wing used for these tests had 30° sweep of the quarter chord, an aspect ratio of 6.6, and was equipped with six pod-mounted engines as shown in figure 2. A cross section of this wing configuration showing the pod-mounted engine, deflector plate, and slotted flap is given in figure 4. No data are presented for the configuration in which the tail pipe was tilted to direct the jet toward the base of the flap. The results obtained from the few tests made with this configuration were in general agreement with the results obtained with the deflector arrangement of figure 4. A comparison of the data of figure 8 show that for a flap deflection of 60° the swept wing gave slightly less lift coefficient and negative pitching moment. The reduction in pitching-moment coefficient is attributed to the decrease in distance from the center of pressure of the flap load to the aerodynamic center of the wing, which was brought about by the inboard location of the jets on the swept wing. The variations of drag coefficient for the two wings show the same general form although the unswept wing had higher values.

Comparison of two-jet and six-jet arrangements.- Data obtained from tests of the swept wing alone to show a comparison of the two-jet and six-jet arrangements are presented in figure 9. The spanwise position of the jets in the two-jet arrangement was halfway between the inboard and middle positions of the six-jet configuration. The data of figure 9 show that the two-jet configuration gave almost as much lift for a given value of C_μ as the six-jet configuration and provided a further reduction in pitching moment.

Effect of flap deflection.- The effect of flap deflection on the aerodynamic characteristics of the complete model is presented in figure 10 for the six-jet configuration and in figure 11 for the two-jet configuration. These data show effects of flap deflection similar to those determined in the tests of the internal-flow jet flap of reference 4; that is, there was an increase in lift coefficient and negative

pitching-moment coefficient as the flap deflection increased. The large negative drag (or thrust) obtained at the smaller flap deflections was reduced as the flap angles increased because of the drag of the wing with a flap and the decrease in the horizontal component of the thrust.

Effect of wing position.- In order to study the effect of wing position on the lift produced by the jet-augmented flap, tests were made with the swept wing mounted in a low and high position on a fuselage. These tests were made with the horizontal tail off to isolate the effects of wing-fuselage interference. The data from these tests, presented in figure 12, show that the high-wing configuration gave about the same lift as the wing alone. The low-wing configuration shows a considerable loss in lift apparently because of a large wing-fuselage interference. This loss in lift evidently occurs over the inboard portion of the wing since it results in a rearward shift in the flap center of pressure as indicated by the increase in negative pitching moment. It is possible that improving the wing-fuselage juncture would bring the data for the low wing into better agreement with the data for the high wing.

Longitudinal Stability and Trim

The data obtained for the longitudinal stability and trim study are presented in figures 13 to 16 and are summarized in figures 17, 18, and 19. The basic data were measured over an angle-of-attack range from -8° to 12° and for a flap deflection of 60°. The 60° flap deflection was chosen for the stability and trim study because the range of flap angles required for zero drag or steady level flight is somewhere near this value for existing jet transport and bomber airplanes. All the pitching-moment data presented in this section are referred to a center-of-gravity location of 40 percent of the mean aerodynamic chord on the basis of the following reasoning: If the center of gravity is located at 25 percent of the mean aerodynamic chord which has been used as a reference point for all the foregoing data, an unreasonably large horizontal tail is required to trim out the pitching moment produced by the jet flap. Such a large tail will move the aerodynamic center so far rearward that the airplane would have an unnecessarily large static longitudinal stability. Obviously, the proper course is to use a somewhat larger tail than that of a conventional airplane. From the use of this larger tail a more rearward aerodynamic center would result so that the center of gravity could be located in a more rearward position; thus, the amount of pitching moment which must be trimmed out would be reduced. Some preliminary analysis of the data indicated that a reasonable relationship of the stability, trim, and horizontal-tail size could be obtained with the center of gravity located at 40 percent of the mean aerodynamic chord. Therefore, the data are referred to this point for convenience in analysis.

The model used for this study was the two-jet high-wing configuration shown in figure 3(b). This configuration was tested with two different size horizontal tails (S_t/S = 0.17 and 0.34) and with two different locations of the horizontal tail on the vertical tail. One location was at the base of the vertical tail (designated low-tail position) and the other at the top of the vertical tail (designated high-tail position). Included in this study was the effect of tail high-lift devices on the longitudinal stability and trim characteristics.

Although these results were obtained with an external-flow jet-augmented flap arrangement, it is felt that they are generally applicable to configurations with other jet-flap arrangements.

Tail-off configuration.- The data for the tail-off configuration are presented in figure 13. These data show that the instability of the model decreases as C_μ increases. This variation in stability with C_μ is similar to that shown in reference 2 and is apparently associated with the increase in lift-curve slope of the wing and the delay in stall angle obtained at the higher values of C_μ.

A comparison of the high-wing data of figure 13 with the data of figure 12 for an angle of attack of 0° shows somewhat lower values of C_L in figure 13 for given values of C_μ. The reason for this difference is not known but it may be related to the fact that, during the time between the running of the two sets of tests, the model was completely dismantled and various parts of the model had been used in other investigations. When the model was reassembled for the stability studies, the wing surfaces were rougher and the geometric characteristics of the slot were probably different from that used in the earlier tests. Unpublished data for the low-wing model in the rough condition also showed values of C_L which were lower than those shown for the earlier low-wing data of figure 12. The lift data shown in figure 13 are therefore considered to be somewhat conservative.

Low-tail position.- Data obtained for the model with the small and large tails in the low position are presented in figure 14. In general, as C_μ is increased, the pitching moments become more negative and the static stability decreases; this condition results in instability over most of the lift-coefficient range. As a result, even the large horizontal tail does not provide both trim and stability at the higher lift coefficients. The data of figure 14(c) show that the model with the large tail at an angle of incidence of 0° was trimmed but was longitudinally stable only at the lower lift coefficients.

High-tail position.- In an effort to increase the longitudinal stability by placing the tail in a more favorable downwash field, the horizontal tail was moved to the top of the vertical tail. The data for

this configuration are presented in figure 15. In general, these data show an increase in stability for a given configuration in going from the low tail (fig. 14) to the high tail (fig. 15). The model with either tail at an incidence of 10° was longitudinally stable over most of the lift-coefficient range but was still untrimmed.

High-lift devices on tail.- Analysis of the data of figures 14 and 15 indicated that the low trimming power of the horizontal tail could be attributed to a relatively low maximum lift coefficient of the tail which resulted from the low scale of the tests. In order to increase the maximum lift coefficient of the tail, leading-edge and trailing-edge flaps were installed on the tails (see fig. 3(b)) and tests were made with the tails in the high position. It is felt that the maximum lift coefficient of the tail with the leading-edge flap in these low-scale tests would be approximately the same as that obtained at full scale without leading-edge flaps. The data obtained with this arrangement, presented in figure 16, indicate that the small tail was not adequate for stability and trim but that the large tail was more than adequate.

Horizontal-tail area required.- In order to indicate the size of the horizontal tail required for longitudinal stability and trim at lift coefficients around 5 or 6, some of the data of figures 13 to 16 have been replotted in figures 17 to 19. The pitching-moment curves for various tail configurations for values of C_μ of 2.20 and 2.95 are presented in figure 17. Tail pitching-moment increments for the same conditions are shown in figure 18. The data from these two figures have been cross-plotted against S_t/S and are presented in figure 19. The data of figure 19 indicate that a horizontal-tail area equal to 25 percent of the wing area provided adequate longitudinal trim with a static margin of about 6 to 8 percent. In order to achieve this result, it was necessary to locate the horizontal tail in a position well above the chord plane of the wing and to incorporate both variable incidence and an elevator. In this investigation elevators were simulated by trailing-edge split flaps.

Flap-up configuration.- In order to determine the longitudinal stability of the high-wing, high-tail model with the flap up, tests were made over an angle-of-attack range with zero thrust. The data from these tests, presented in figure 20, show that the model had about 10 percent static margin with the small tail and about 40 percent static margin with the large tail for a center-of-gravity location at 40 percent of the mean aerodynamic chord. Interpolation of these results indicates that the horizontal-tail area equal to 25 percent of the wing area would provide about 25 percent static margin for the flap-up condition.

Estimated Take-Off and Landing Performance

Before making estimates of the take-off and landing performance of an airplane with an external-flow jet-augmented flap, it is necessary to consider the thrust lost in spreading and deflecting the jet. As stated previously all the data presented herein for flap deflections of 60° have been corrected by a factor of 25 percent (determined from static calibrations) to allow for this loss. It is believed, however, that in a refined full-scale application these losses might be less than those determined in the small-scale tests of the present investigation. In order to indicate the effects of these losses on performance, the lift data used in performance estimates are presented for no thrust loss as well as for the 25-percent loss. It is felt that in actual airplane applications the losses caused by spreading and deflecting the jet will fall somewhere between these two values.

Presented in figure 21 are lift data for the high-wing, high-tail model which is a stable and trimmed configuration. The dashed lines represent thrust-weight ratios of 0.1, 0.2, 0.3, 0.4, and 1.0. The intersections of the dashed and solid lines determine the lift coefficient available for a given thrust-weight ratio. These data, which were taken from figure 16, were obtained for a flap deflection of 60°. With this flap deflection, zero drag is obtained at a fairly high lift coefficient representative of the landing condition. For take-off, a lower flap deflection would be required to obtain zero (or negative) drag at the lower lift coefficients that could be obtained in this condition. The data of figure 10 indicate that reducing the flap deflection from 60° to 50° provides a substantial increase in thrust without a large loss in lift. For the purpose of these rough preliminary calculations, therefore, the data of figure 21 will be used to calculate take-off speeds as well as landing speeds.

The data of figure 21 are replotted in figure 22 in terms of lift coefficient against thrust-weight ratio. The upper two curves are the data for the jet-augmented flap configuration and the lower curve represents the lift available with the jet thrust directed downward for direct lift (not to supply a jet-augmented flap). Comparison of these data at any given thrust-weight ratio indicates that the jet-augmented flap makes much more efficient use of the available jet thrust. Symbols have been plotted on the jet-augmented flap curves at average values of thrust-weight ratio for current jet transport and jet bomber designs. The value of thrust-weight ratio for take-off estimates was 0.25 and gives lift coefficients of about 3 to 3.5. The value of thrust-weight ratio used for landing estimates was 0.40 and gives lift coefficients of about 4.5 to 5.7. These lift coefficients were used to determine the minimum take-off and landing speeds for assumed wing loadings of 110 to 70 pounds per square foot and the results are presented in figure 23.

The results of figure 23 show that the landing speed with the jet-augmented flap is about 60 knots compared with a speed of about 100 knots without the jet-augmented flap. The right side of the plot shows that the take-off speed with the jet-augmented flap is about 100 knots compared with a speed of about 150 knots without the jet-augmented flap. All the take-off and landing speeds shown in figure 23 are for steady flight and are the minimum speeds for the conditions assumed. In all cases, the operational speeds in a practical application would be somewhat higher.

These reductions in minimum speed lead to large improvements in take-off and landing distance because these distances vary roughly as the square of the speed. Based on the lift coefficients shown in figure 23, it is estimated for existing jet transport and bomber airplanes that the landing and take-off distances could be cut approximately in half. These reductions in take-off and landing speed and distance were calculated on the assumption that the full installed thrust of the engines will be available. The extent to which these values can be realized in actual practice will depend upon the number of engines and the extent to which they can be relied upon during take-offs and landings. Another factor which should be considered in detailed calculations of take-off and landing performance is the effect of ground interference. The results of reference 1 and certain unpublished data have indicated that such effects can be appreciable especially for low-wing configurations.

SUMMARY OF RESULTS

The results of the wind-tunnel investigation of the external-flow jet-augmented slotted flap may be summarized as follows:

1. The external-flow jet-augmented flap produced values of circulation lift large enough to warrant serious consideration of its use for increasing the maximum lift coefficients of airplanes with pod-mounted jet engines. This jet flap, however, was not as effective in producing circulation lift as the internal-flow jet flap.

2. The results indicated that static longitudinal stability and trim up to lift coefficients of at least 6 could be achieved with a jet transport or bomber airplane equipped with a jet-augmented flap and having a horizontal-tail area equal to 25 percent of the wing area. In order to achieve this result, it was necessary to locate the horizontal tail in a position well above the chord plane of the wing and to incorporate both variable incidence and an elevator.

3. The results indicated that an external-flow jet-augmented flap applied to existing jet transport and bomber airplanes with pod-mounted

engines would produce lift coefficients of about 3 for take-off (thrust-weight ratio of 0.25) and lift coefficients of about 5 for landing (thrust-weight ratio of 0.40). These lift coefficients would provide substantial reductions in take-off and landing speeds and distances if the full installed thrust of the engines is available. The extent of the reductions which can be realized in actual practice will depend upon the number of engines and the extent to which they can be relied upon during take-offs and landings.

Langley Aeronautical Laboratory,
National Advisory Committee for Aeronautics,
Langley Field, Va., September 14, 1956.

REFERENCES

1. Dimmock, N. A.: An Experimental Introduction to the Jet Flap. National Gas Turbine Establishment Rep. No. R.175, British Ministry of Supply, Apr. 1955.

2. Williams, J., and Alexander, A. J.: Three-Dimensional Wind-Tunnel Tests of a 30° Jet Flap Model. Rep. No. F.M. 2326, British N.P.L. (Rep. No. 17,990, A.R.C.), Nov. 1955.

3. Malavard, L., Poisson-Quinton, Ph., and Jousserandot, P.: Recherches Théoriques et Expérimentales Sur le Contrôle de Circulation Par Soufflage Appliqué aux Ailes D'Avions. O.N.E.R.A. Note Tech. No. 37, 1956. (Available in English translation as Rep. No. 358, Princeton Univ., Dept. Aero. Eng.)

4. Lockwood, Vernard E., Turner, Thomas R., and Riebe, John M.: Wind-Tunnel Investigation of Jet-Augmented Flaps on a Rectangular Wing to High Momentum Coefficients. NACA TN 3865, 1956.

5. Lowry, John G., and Vogler, Raymond D.: Wind-Tunnel Investigation at Low Speeds To Determine the Effect of Aspect Ratio and End Plates on a Rectangular Wing With Jet Flaps Deflected 85°. NACA TN 3863, 1956.

TABLE I.- DIMENSIONAL CHARACTERISTICS OF THE MODELS TESTED

(a) Unswept-Wing Model

Area, sq ft	2.67
Aspect ratio	6.0
Mean aerodynamic chord, ft	0.667
Airfoil section	NACA 0012
Flap chord, percent wing chord	0.25
Taper ratio	1.0
Span, ft	4.00

(b) Swept-Wing Jet Transport Model

Wing:	
Area, sq ft	3.07
Aspect ratio	6.62
Mean aerodynamic chord, ft	0.732
Airfoil section, root	NACA 65_1-414
Airfoil section, tip	NACA 65-410
Flap chord, percent wing chord	0.25
Flap span, percent wing span	1.00
Root chord, ft	1.00
Tip chord, ft	0.367
Span, ft	4.50
Taper ratio	0.367
Sweep of quarter chord, deg	30
Horizontal tail (small):	
Area (total), sq ft	0.53
Length (distance from 0.40$\bar{c}$ of wing to 0.25$\bar{c}$ of tail):	
Low position, wing chords	2.52
High position, wing chords	2.75
Span, ft	1.58
Root chord, ft	0.52
Tip chord, ft	0.15
Mean aerodynamic chord, ft	0.38
Aspect ratio	4.72
Sweep of leading edge, deg	38
Taper ratio	0.321
Airfoil section	NACA 65-009
Horizontal tail (large):	
Total area, sq ft	1.06
Length (distance from 0.40$\bar{c}$ of wing to 0.25$\bar{c}$ of tail):	
Low position, wing chords	2.68
High position, wing chords	2.91
Span, ft	2.33
Root chord, ft	0.62
Tip chord, ft	0.29
Mean aerodynamic chord, ft	0.473
Aspect ratio	5.15
Sweep of leading edge, deg	32
Taper ratio	0.47
Airfoil section	NACA 65-009
Vertical tail:	
Exposed area, sq ft	0.44
Exposed span, ft	0.96
Root chord at fuselage intersection, ft	0.750
Tip chord, ft	0.17
Sweep of leading edge, deg	42
Airfoil section	NACA 65-009

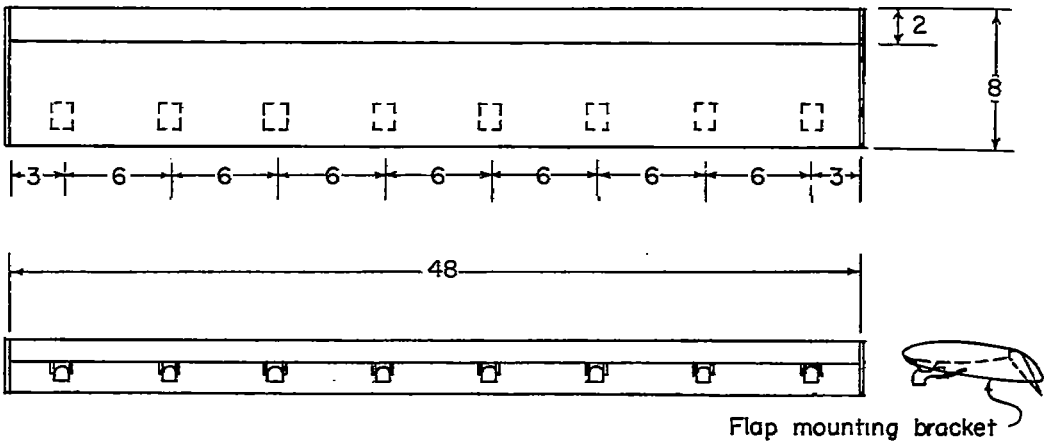

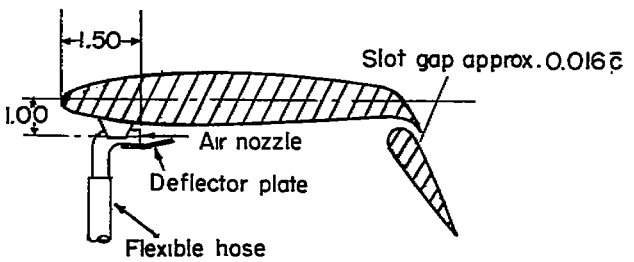

Cross section of wing showing slotted flap

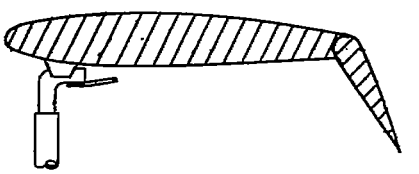

Cross section of wing showing plain flap

Figure 1.- Unswept wing with simulated external-flow jet-augmented flap installed. All dimensions are in inches.

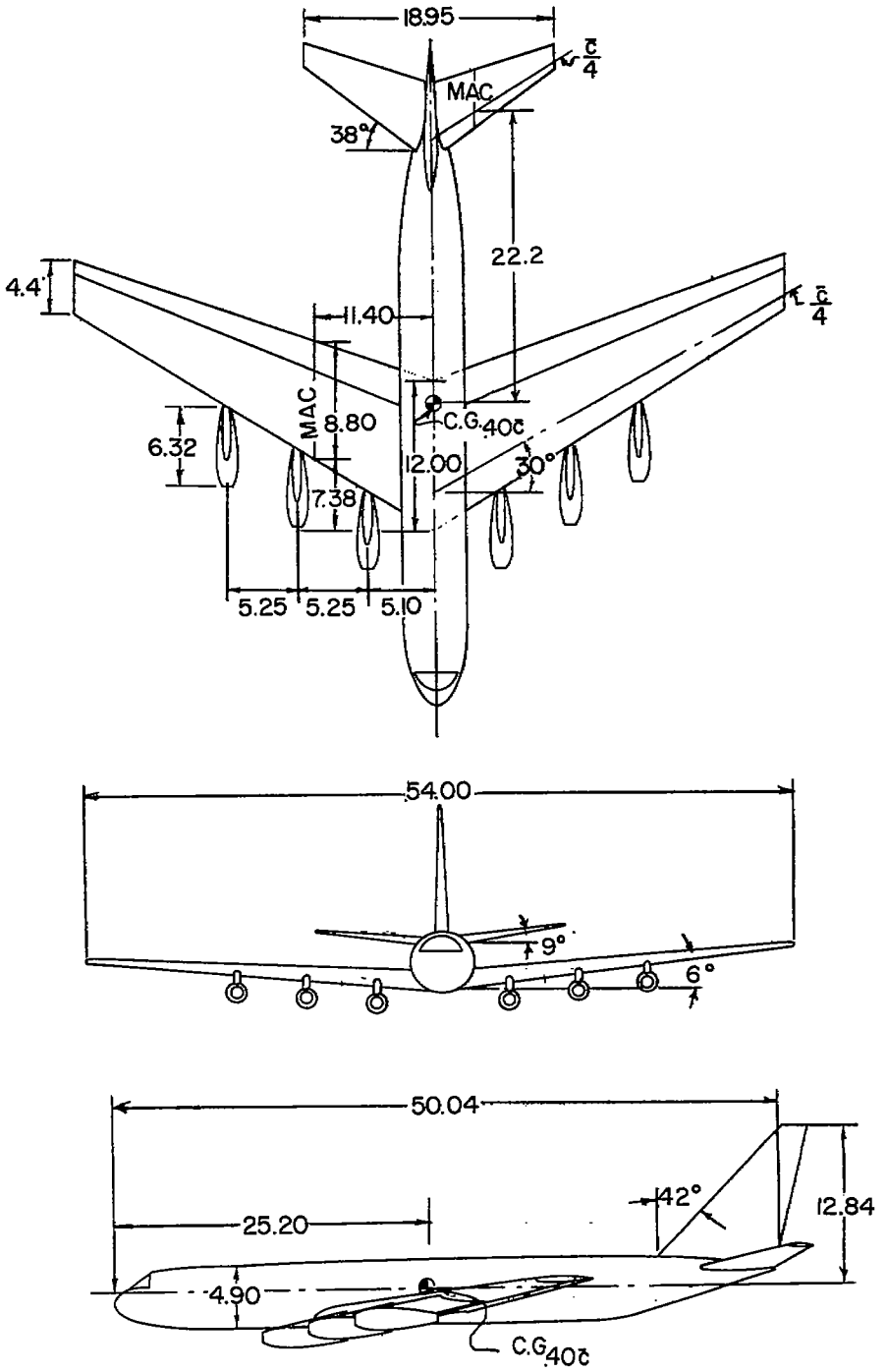

Figure 2.- Six-jet configuration of the swept-wing jet transport model. All dimensions are in inches.

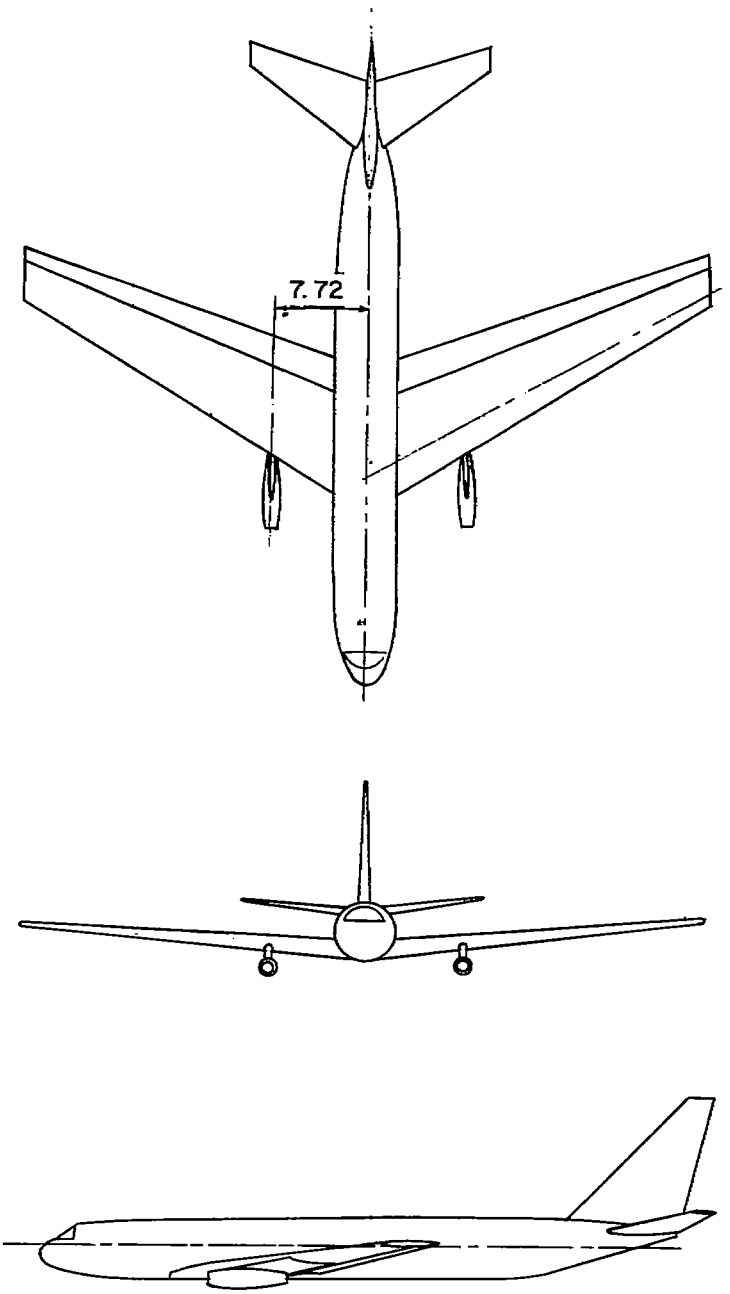

(a) Low-wing configuration.

Figure 3.- Two-jet arrangements of the swept-wing jet transport model. Geometric characteristics of model are the same as those of figure 2 except as noted. All dimensions are in inches.

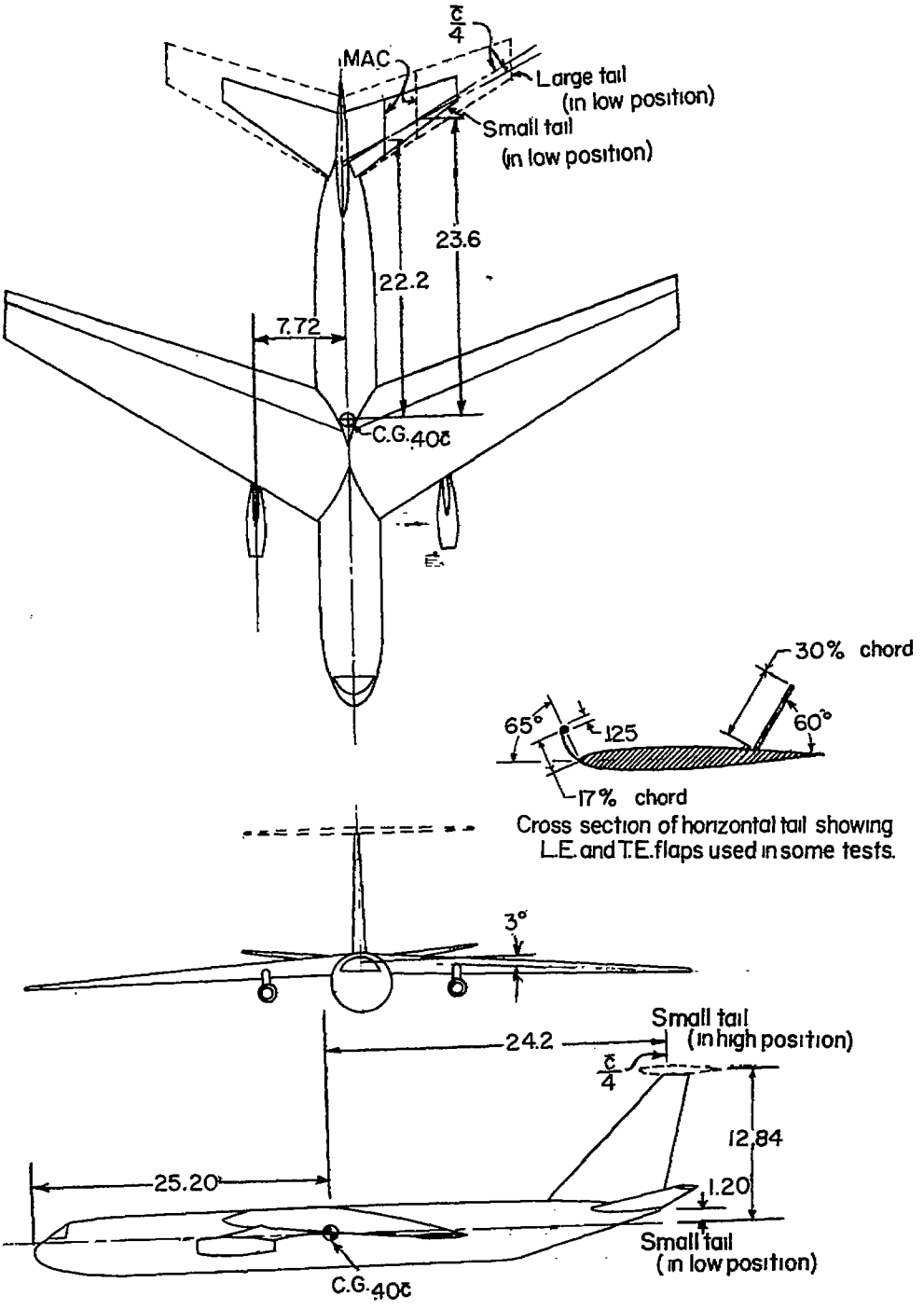

(b) High-wing configuration.

Figure 3.- Concluded.

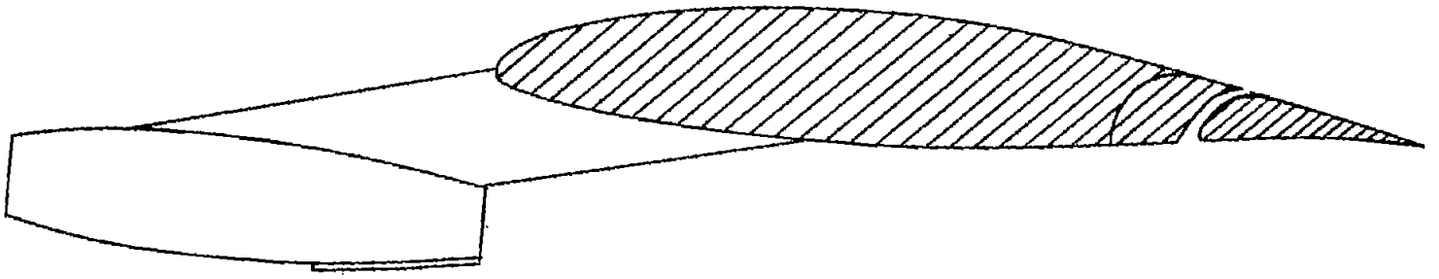

(a) Cross section of wing for cruising-flight condition.

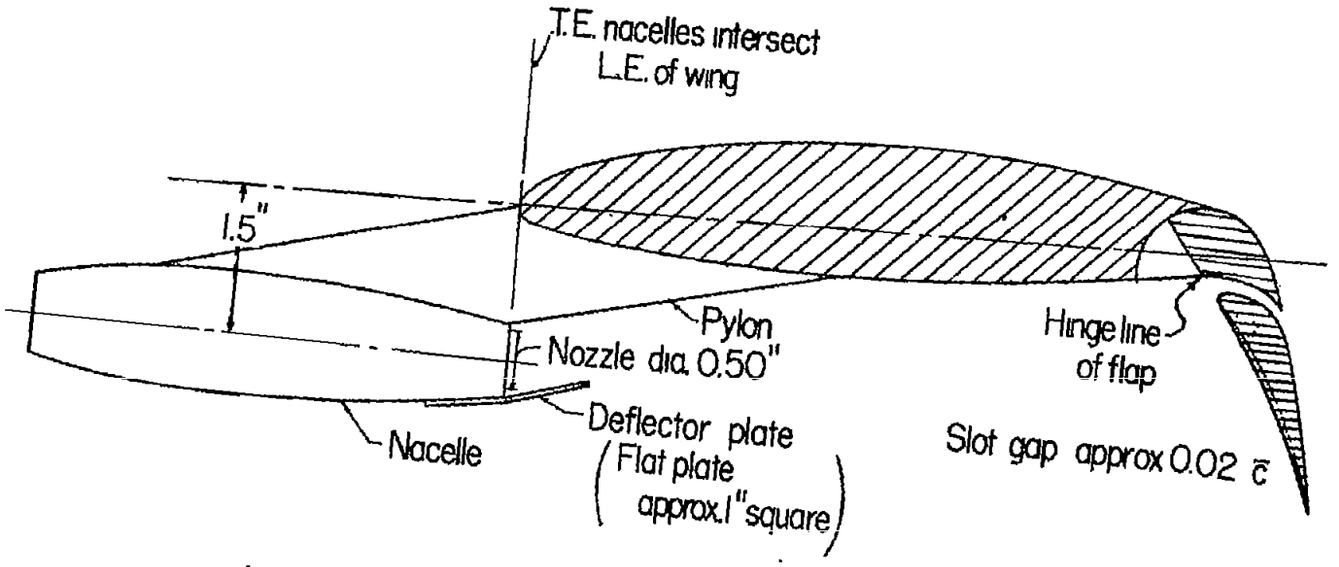

(b) Cross section of wing for landing condition.

Figure 4.- Arrangement of external-flow jet-augmented slotted flap used on swept-wing jet transport models.

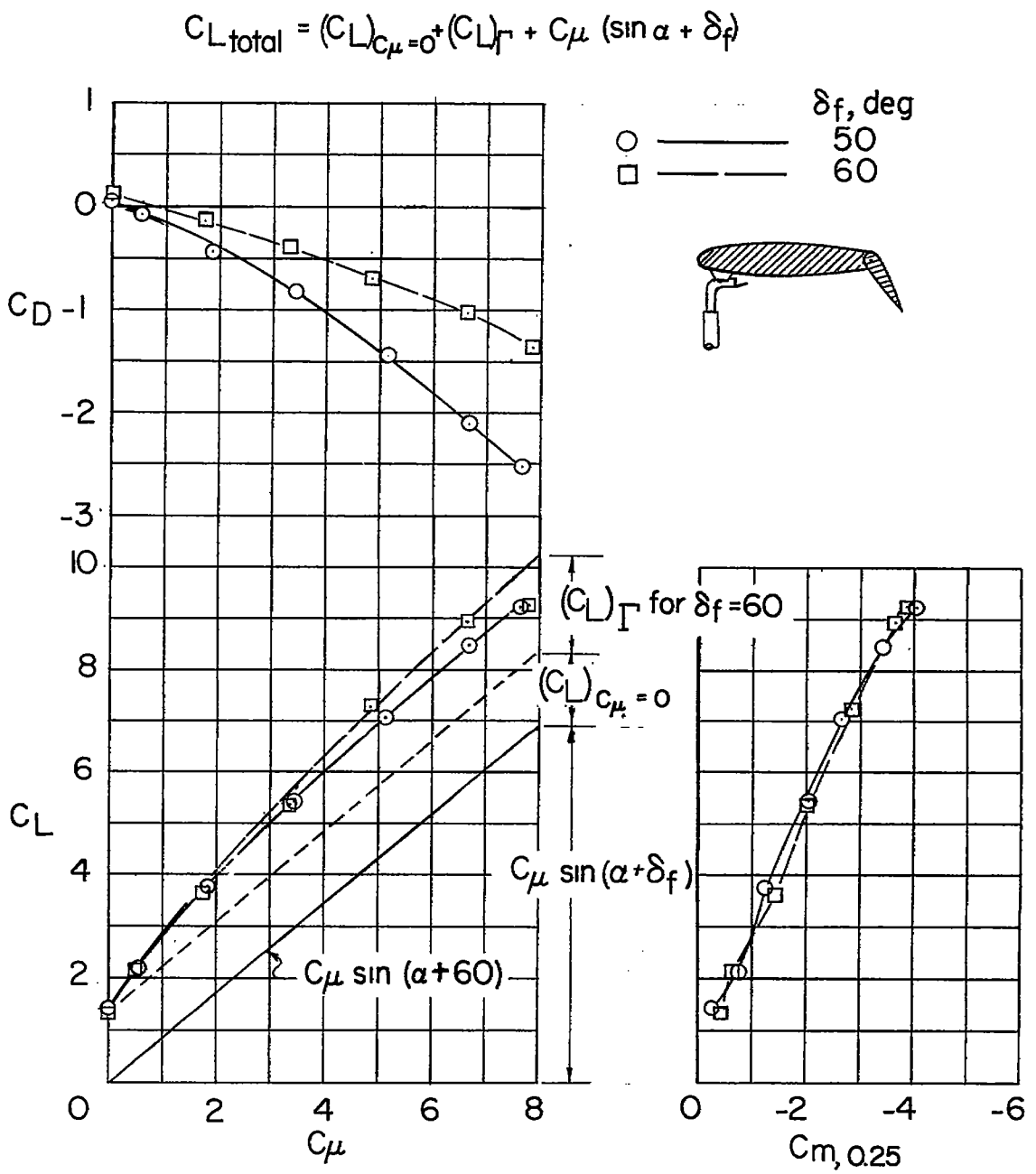

Figure 5.- Effect of simulated external-flow jet-augmented plain flap on the aerodynamic characteristics of the unswept wing. $\alpha = 0^\circ$.

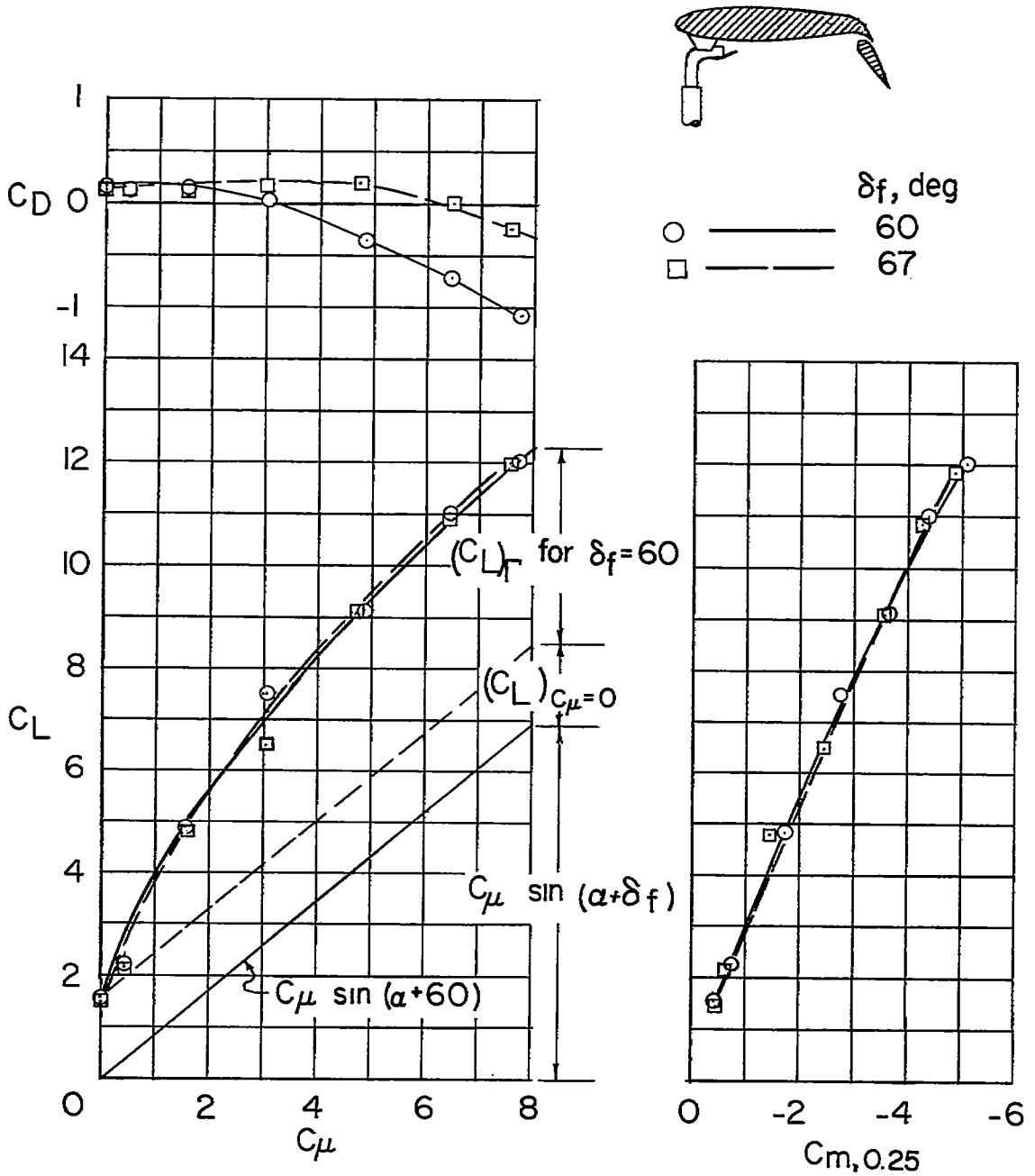

Figure 6.- Effect of simulated external-flow jet-augmented slotted flap on the aerodynamic characteristics of the unswept wing. $\alpha = 0^\circ$.

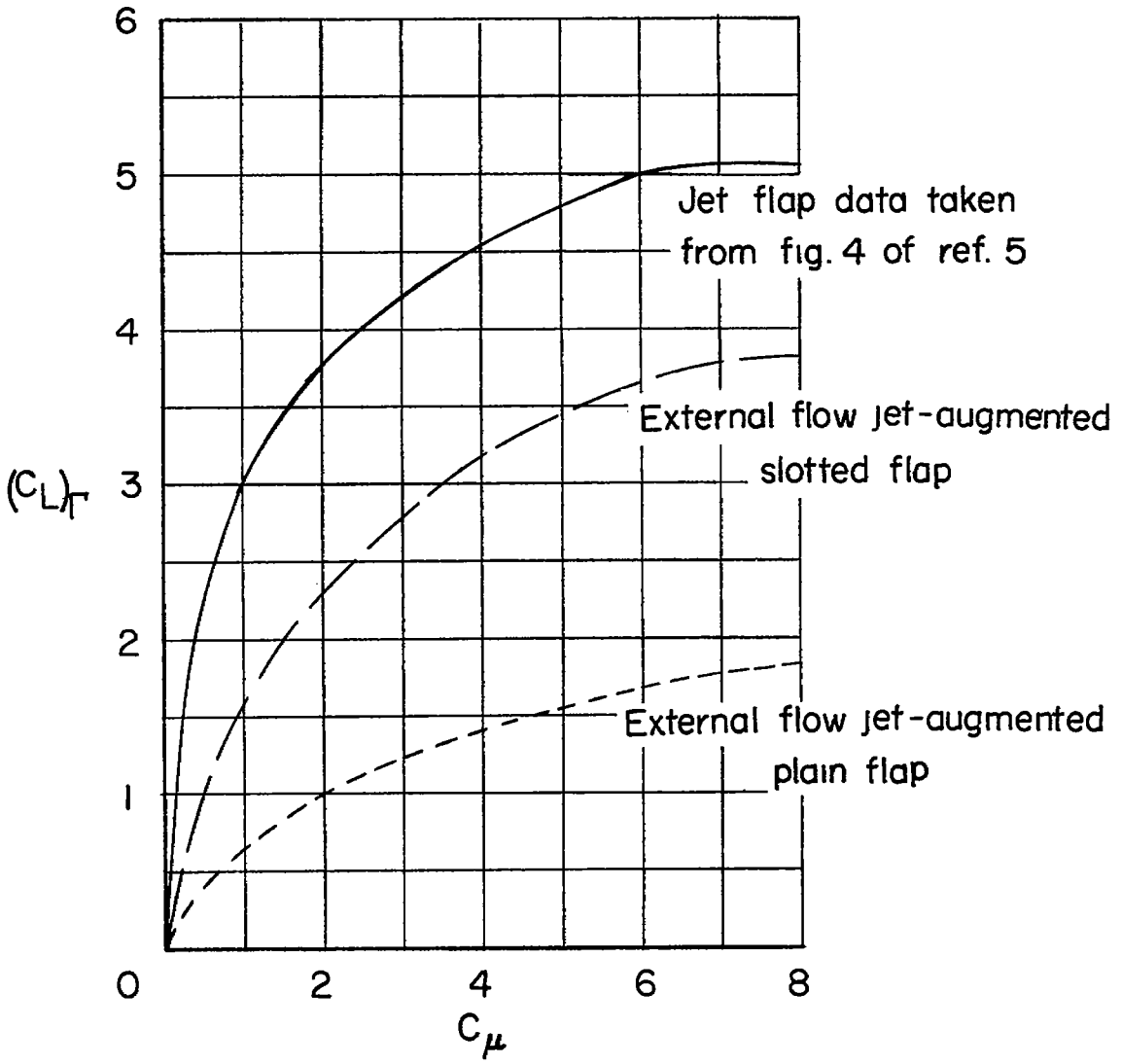

Figure 7.- Circulation lift of external-flow jet-flap arrangements compared with data from reference 5 for an internal-flow type of jet-augmented flap. $\alpha = 0^\circ$; $\delta_f = 60^\circ$.

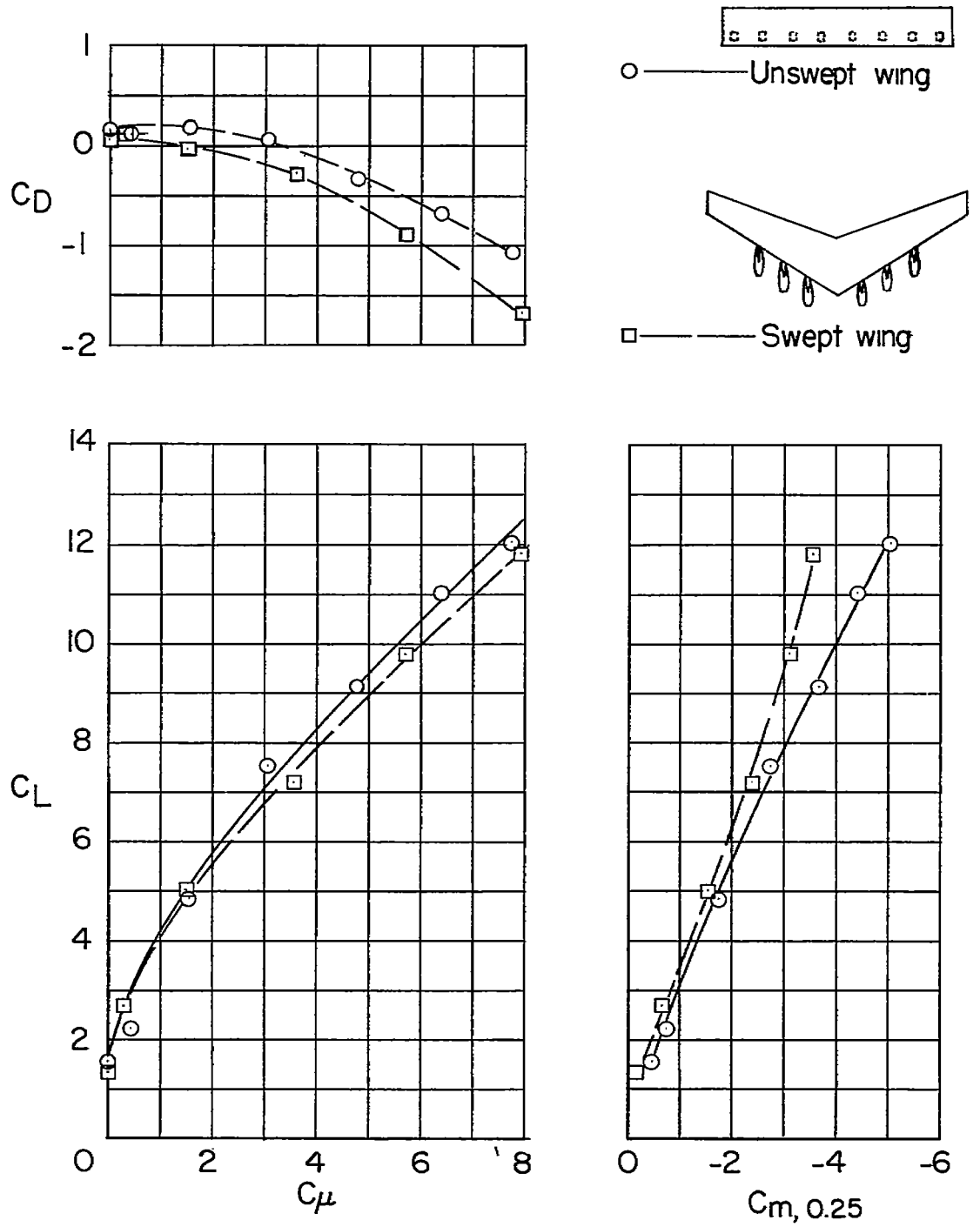

Figure 8.- Comparison of aerodynamic characteristics obtained with swept and unswept wings. $\alpha = 0^\circ$; $\delta_f = 60^\circ$; slotted-flap arrangement.

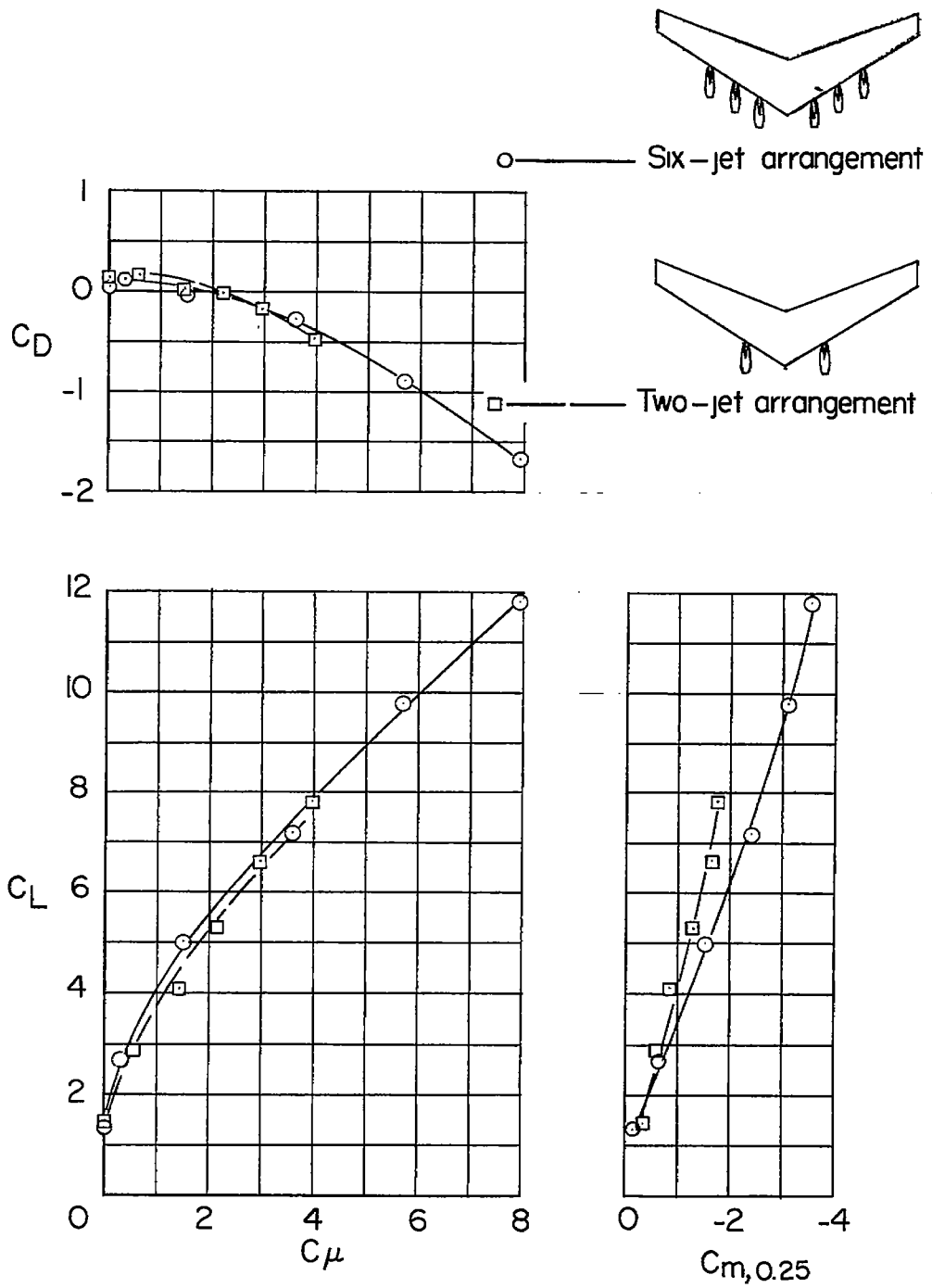

Figure 9.- Comparison of aerodynamic characteristics of the six-jet and two-jet arrangements on the swept wing. $\alpha = 0^\circ$; $\delta_f = 60^\circ$.

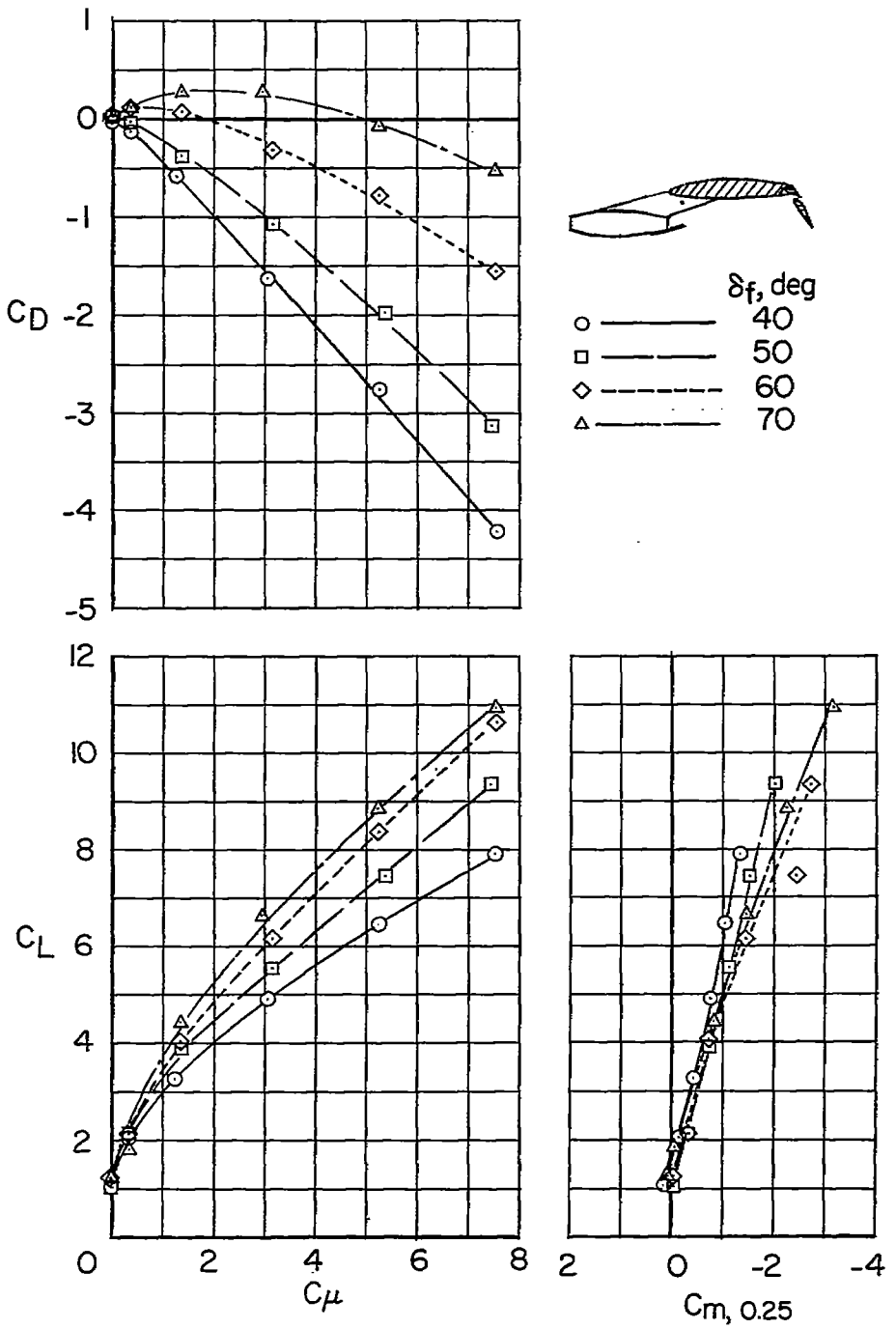

Figure 10.- Effect of flap deflection on the aerodynamic characteristics of the six-jet swept-wing model. Low-wing configuration; low-tail arrangement; $S_t/S = 0.17$; $\alpha = 0^\circ$.

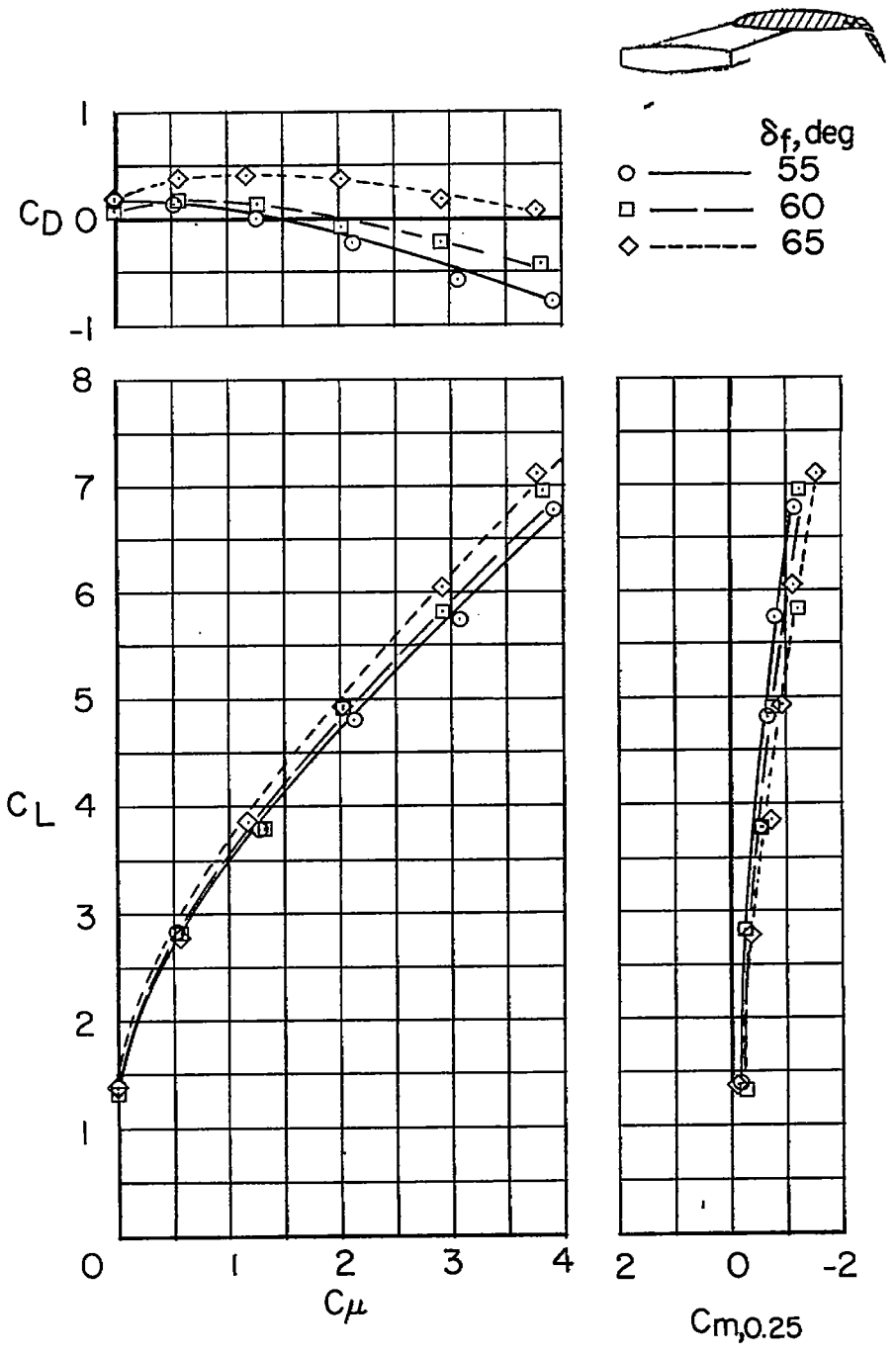

Figure 11.- Effect of flap deflection on the aerodynamic characteristics of the two-jet swept-wing model. Low-wing configuration; low-tail arrangement; $S_t/S = 0.17$; $\alpha = 0^\circ$.

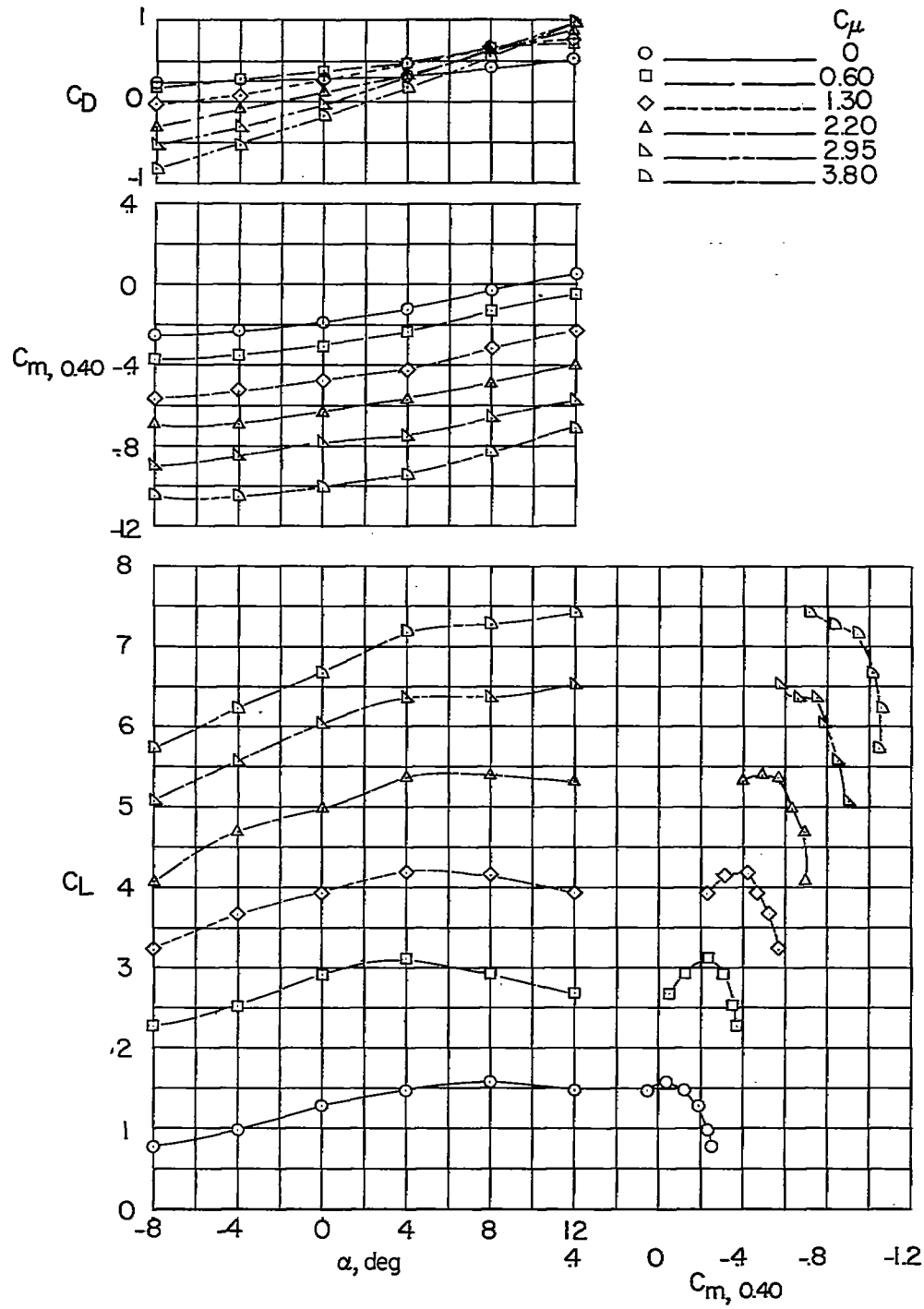

Figure 13.- Longitudinal stability and trim characteristics of the high-wing two-jet swept-wing model. Horizontal tail off.

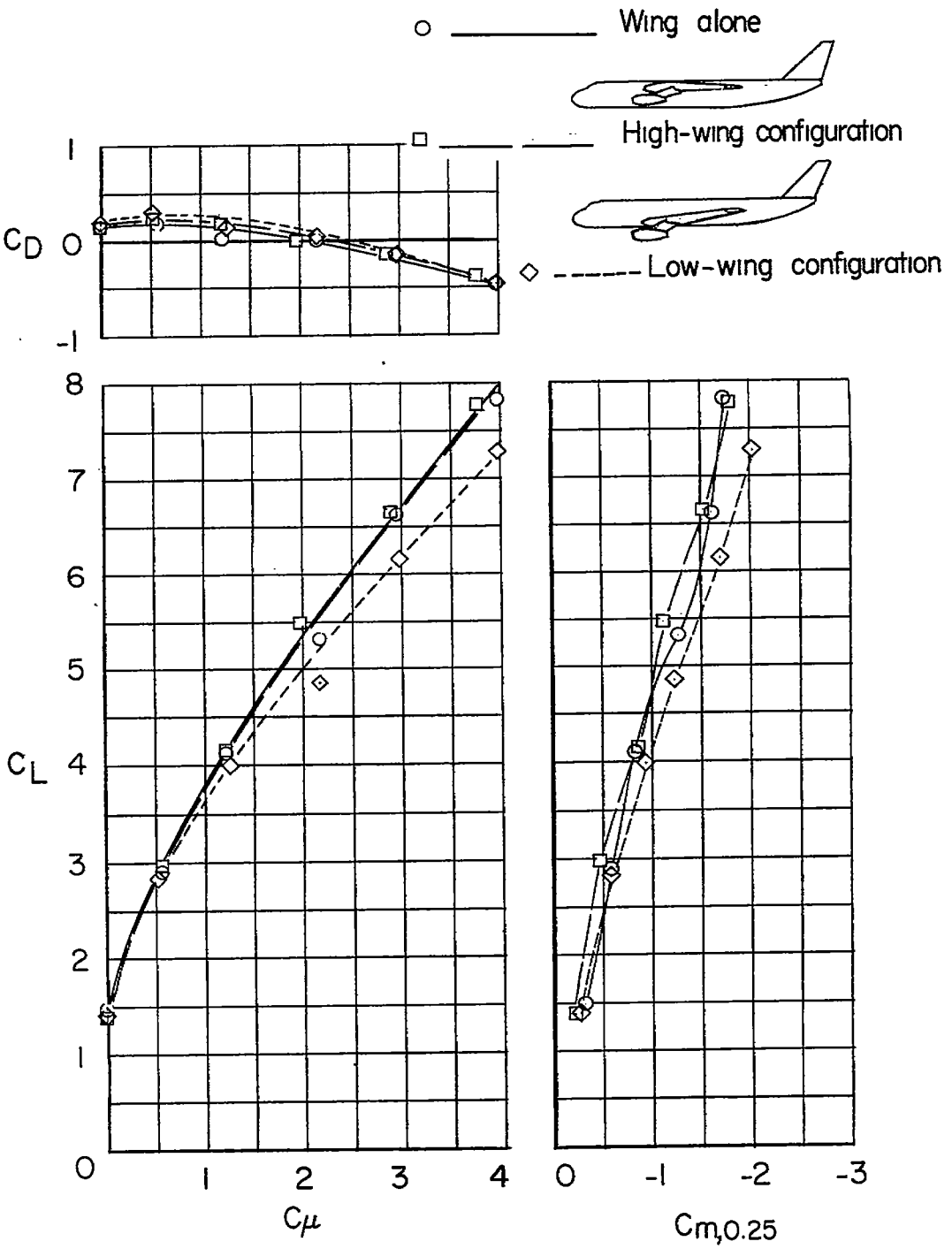

Figure 12.- Effect of wing position on the aerodynamic characteristics of the swept-wing model with two jets. Horizontal tail off; $\delta_f = 60^\circ$.

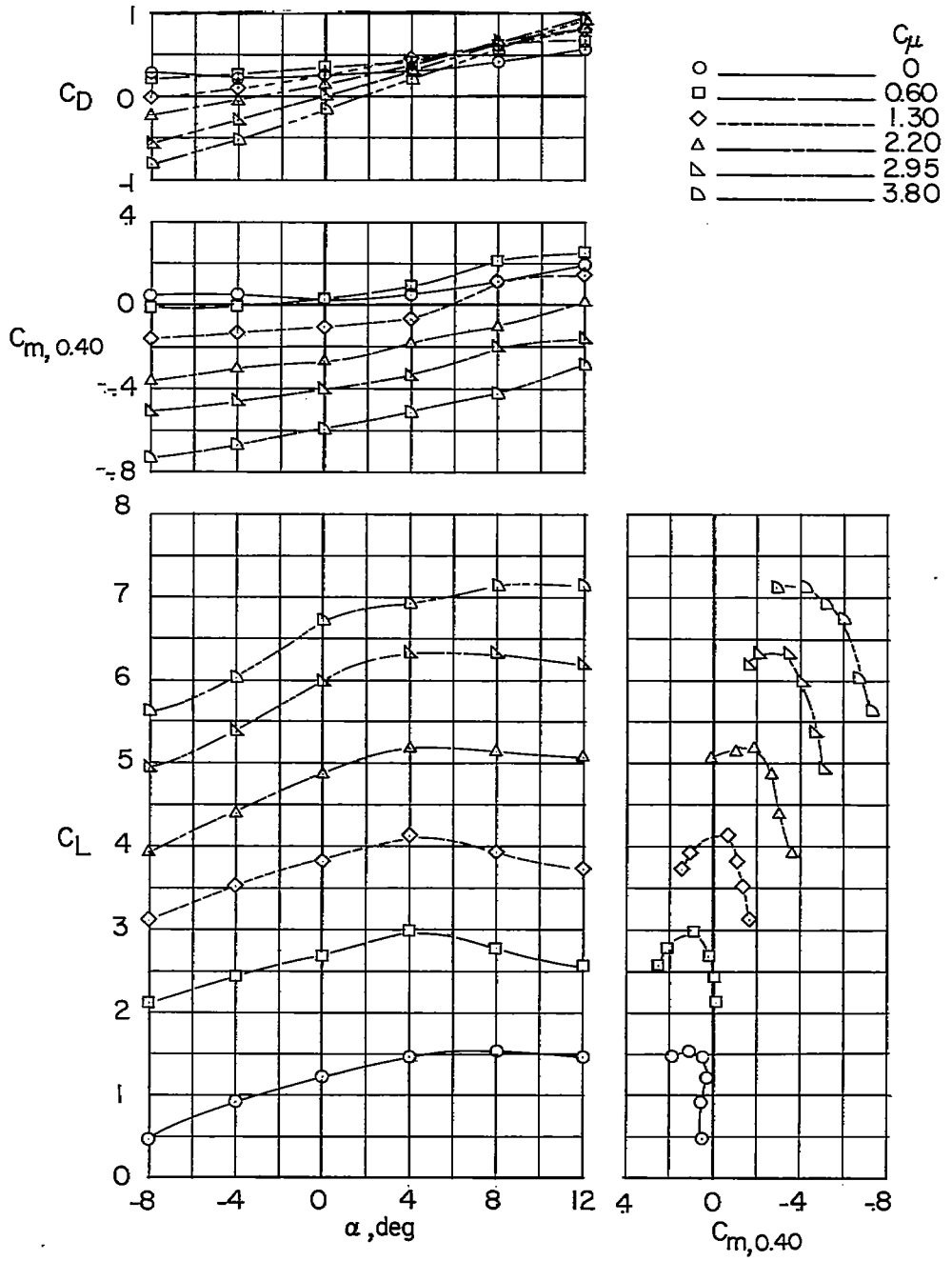

(a) $S_t/S = 0.17$; $i_t = 0^\circ$.

Figure 14.- Longitudinal stability and trim characteristics of the high-wing two-jet swept-wing model. Low-tail arrangement; $\delta_f = 60^\circ$.

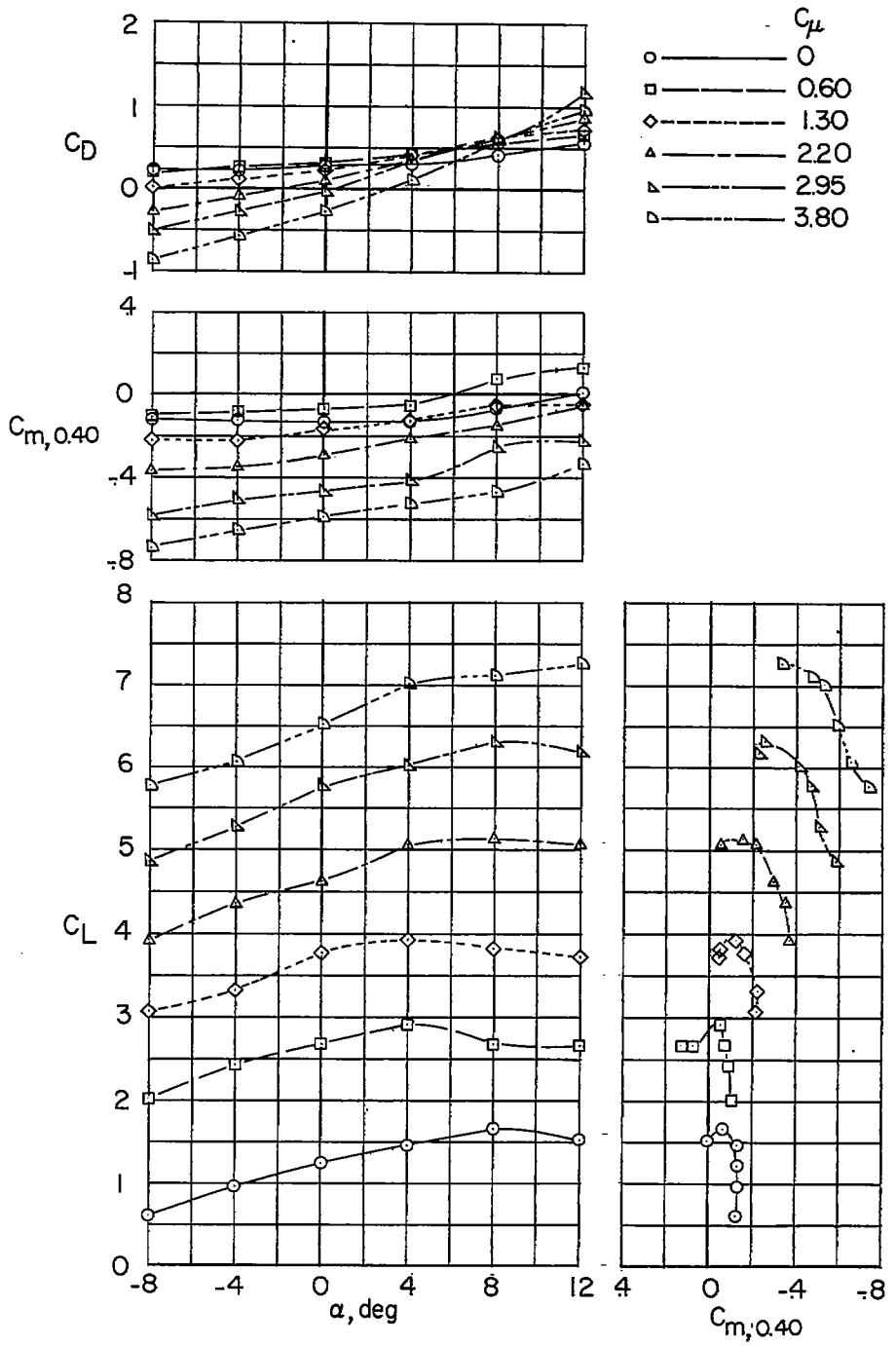

(b) $S_t/S = 0.17$; $i_t = 10°$.

Figure 14.- Continued.

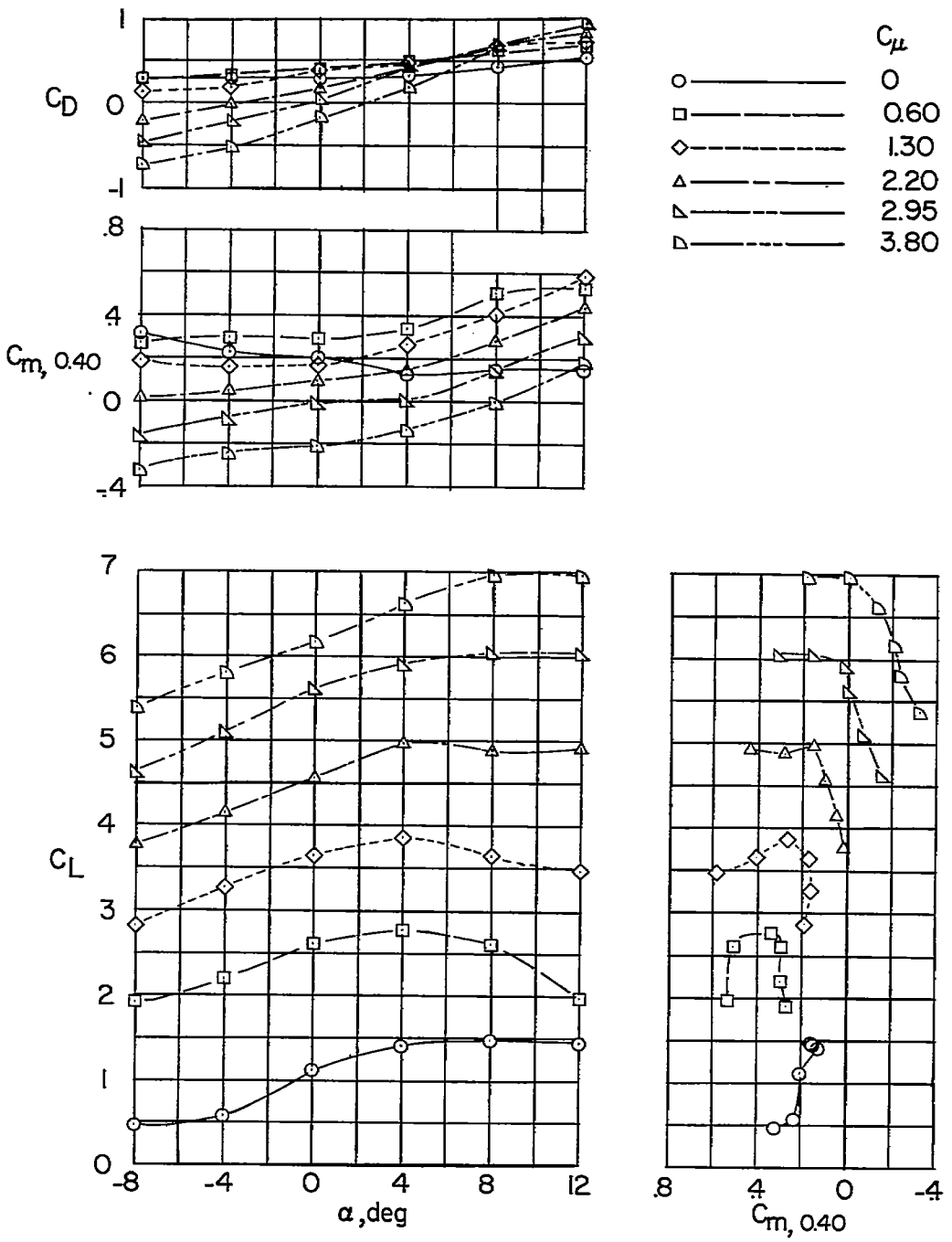

(c) $S_t/S = 0.34$; $i_t = 0°$.

Figure 14.- Continued.

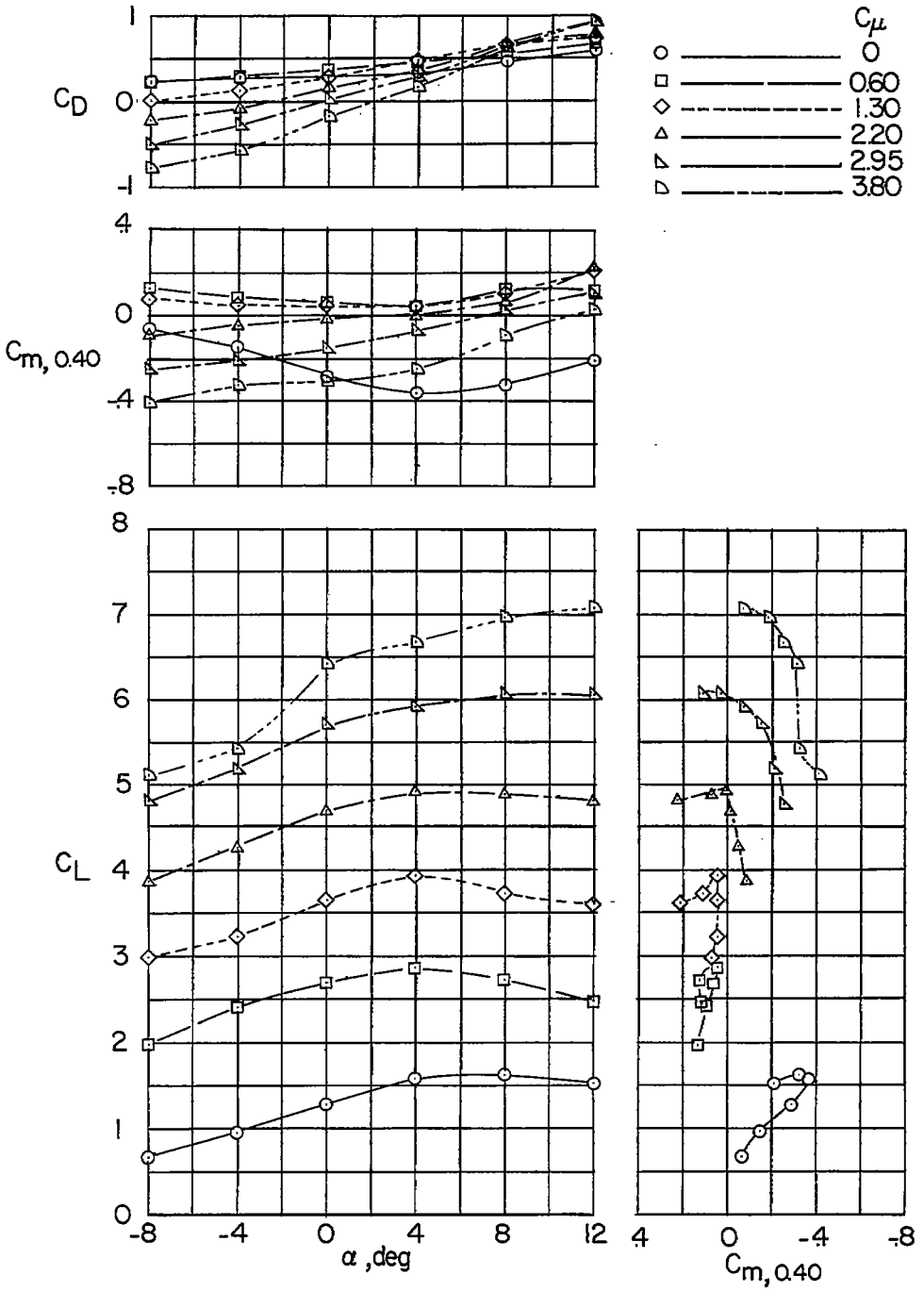

(d) $S_t/S = 0.34$; $i_t = 10°$.

Figure 14.- Concluded.

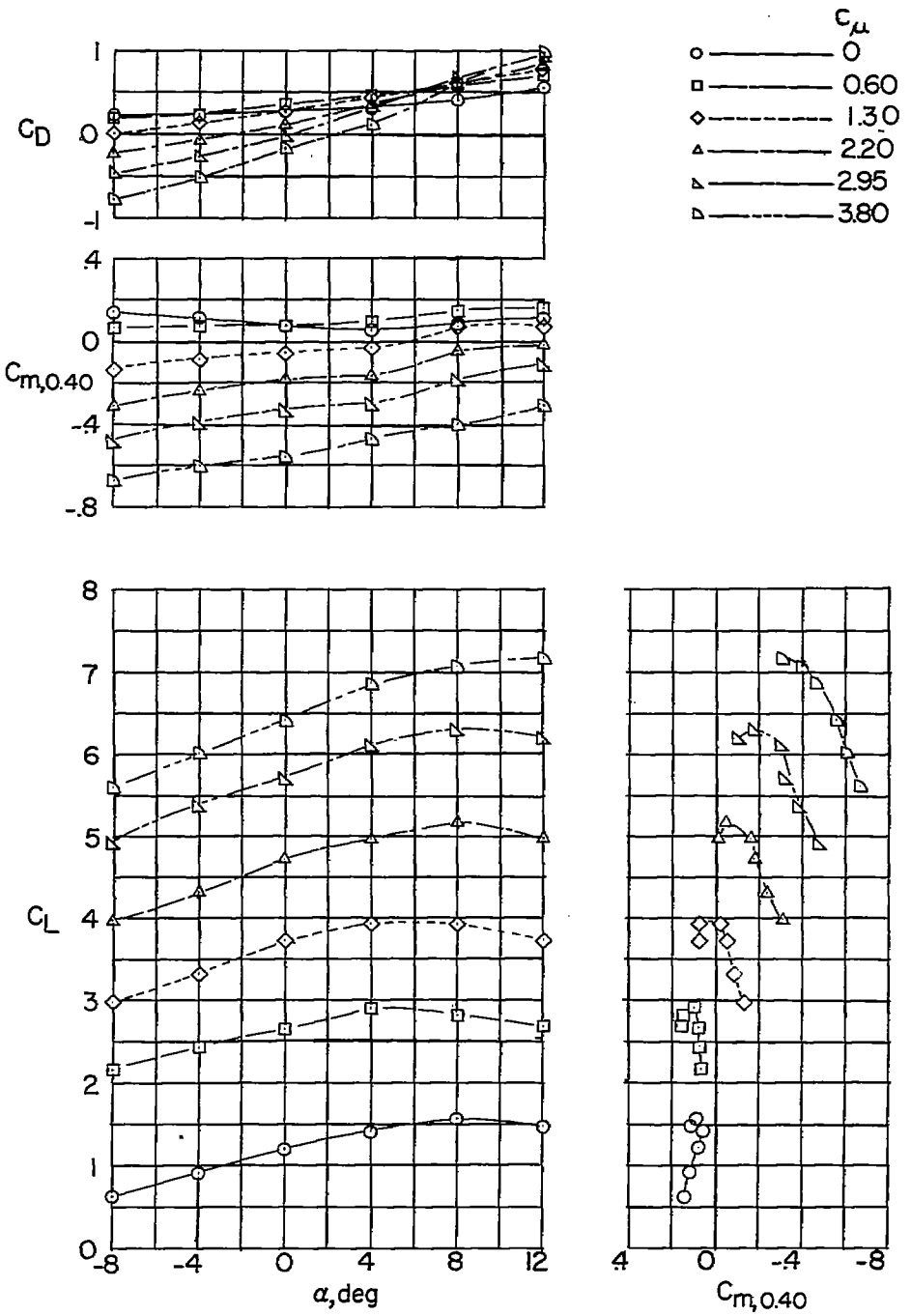

(a) $S_t/S = 0.17$; $i_t = 0^\circ$.

Figure 15.- Longitudinal stability and trim characteristics of the high-wing two-jet swept-wing model. High-tail arrangement; $\delta_f = 60^\circ$.

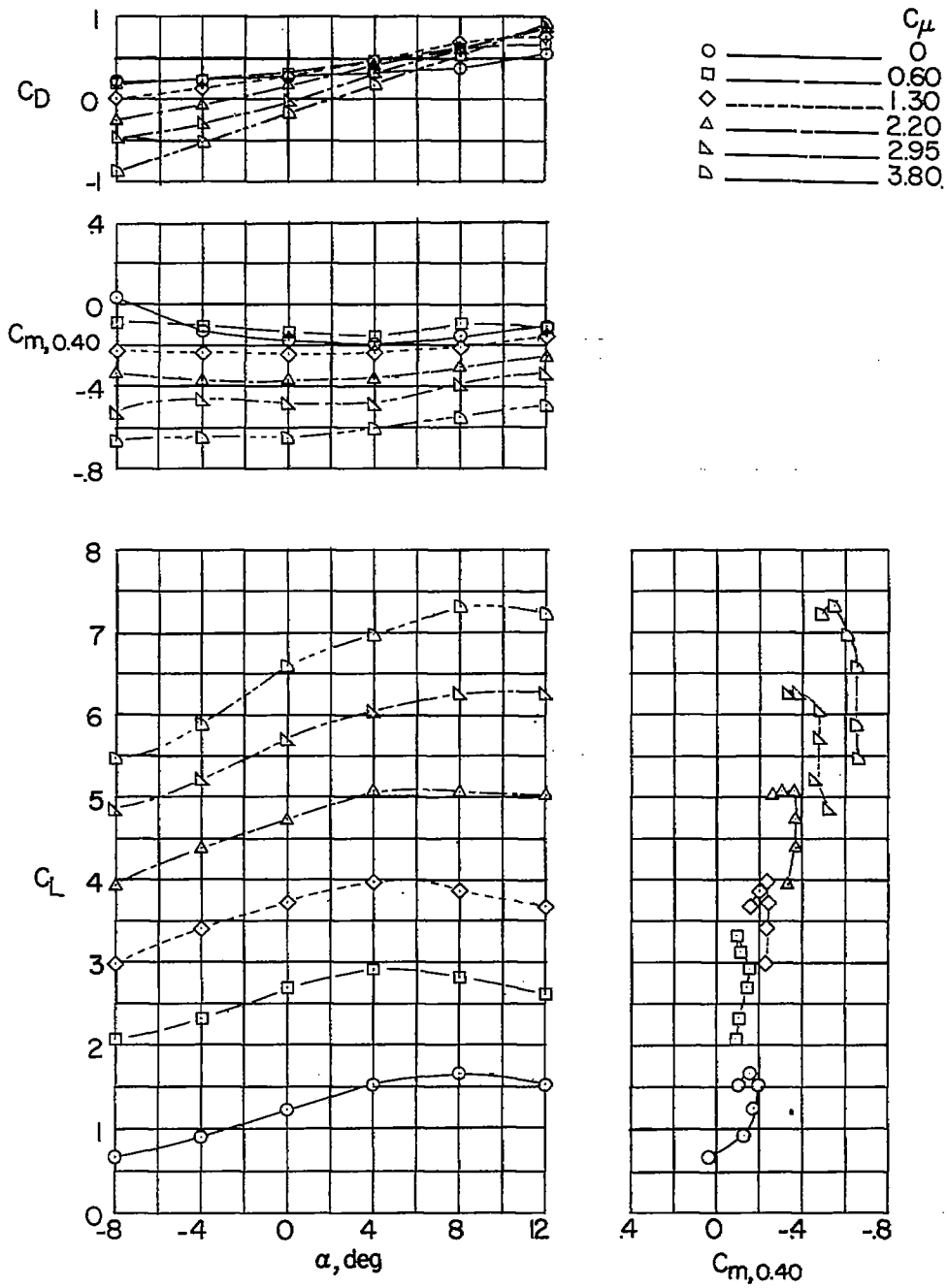

(b) $S_t/S = 0.17$; $i_t = 10°$.

Figure 15.- Continued.

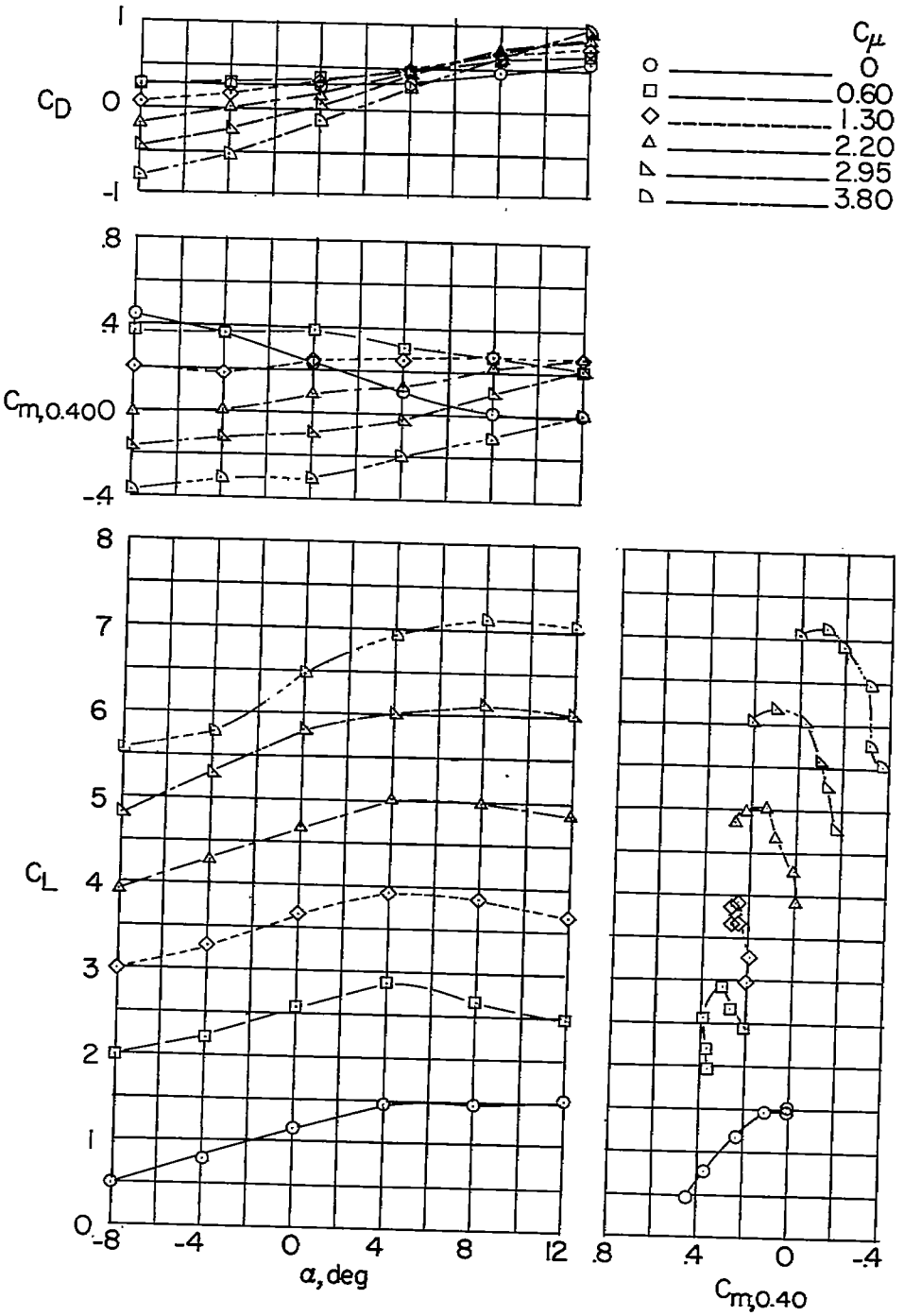

(c) $S_t/S = 0.34$; $i_t = 0°$.

Figure 15.- Continued.

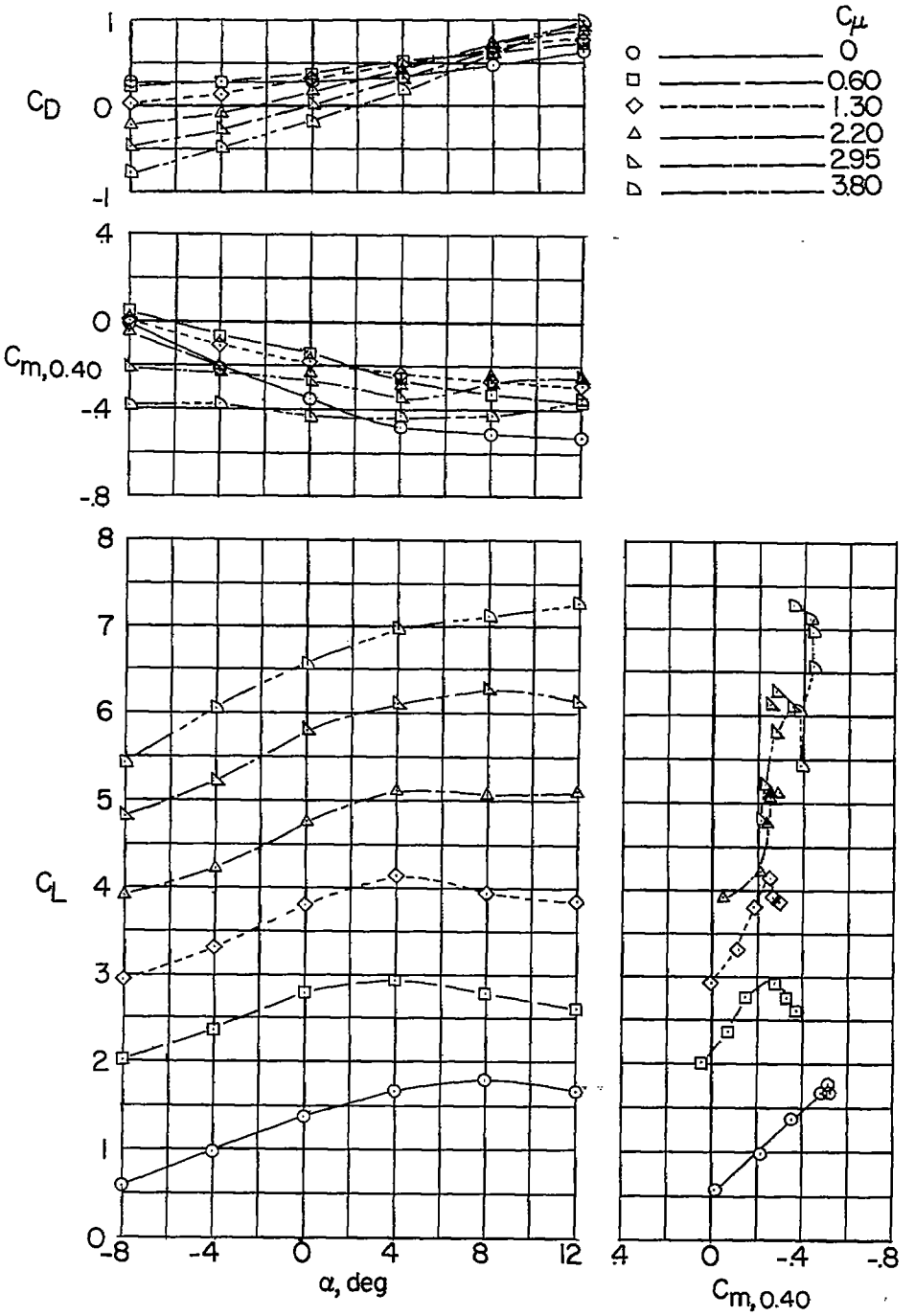

(d) $S_t/S = 0.34$; $i_t = 10°$.

Figure 15.- Concluded.

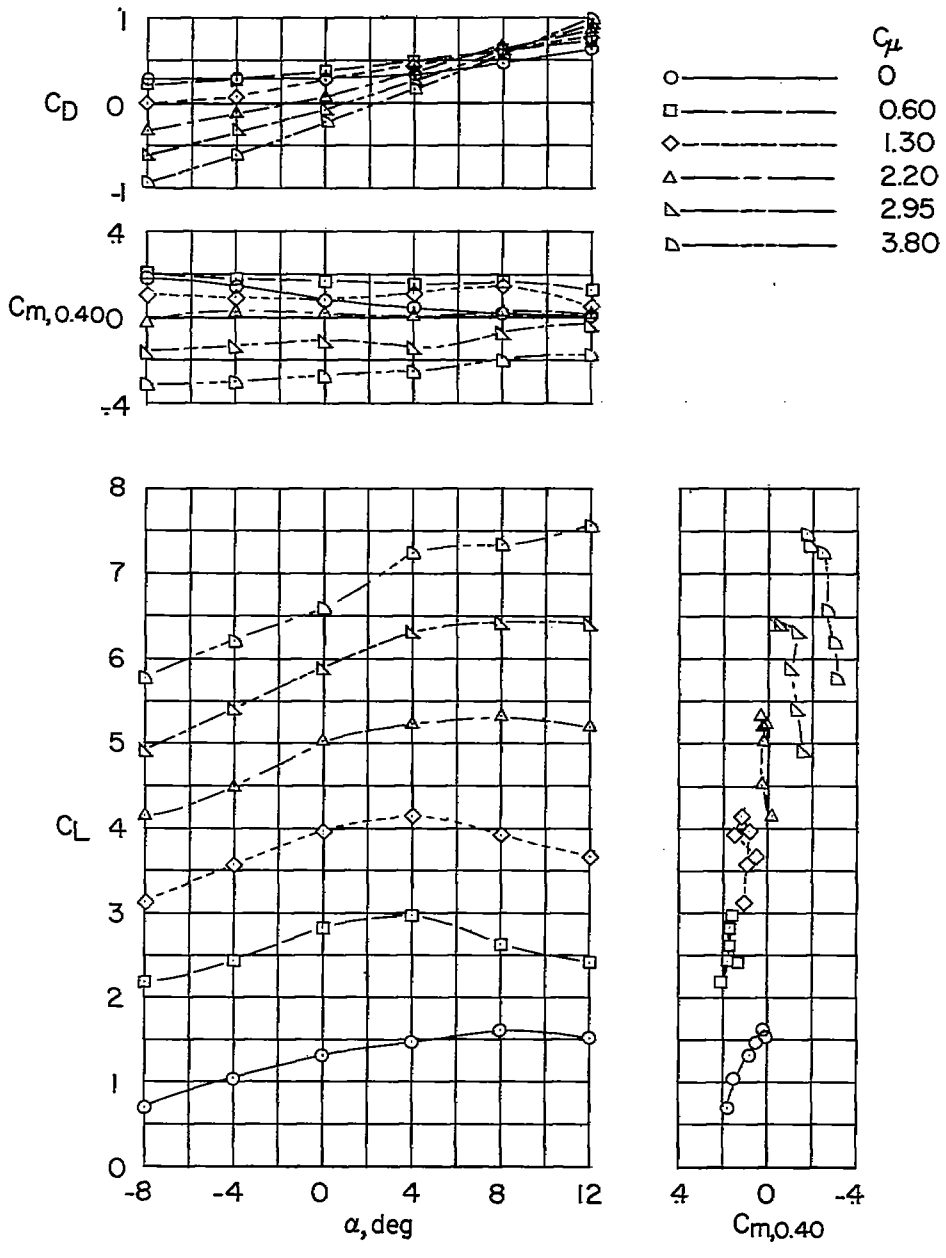

(a) $S_t/S = 0.17$; $i_t = 10^\circ$.

Figure 16.- Longitudinal stability and trim characteristics of the high-wing two-jet swept-wing model. High-tail arrangement; leading- and trailing-edge flaps on the horizontal tail; $\delta_f = 60^\circ$.

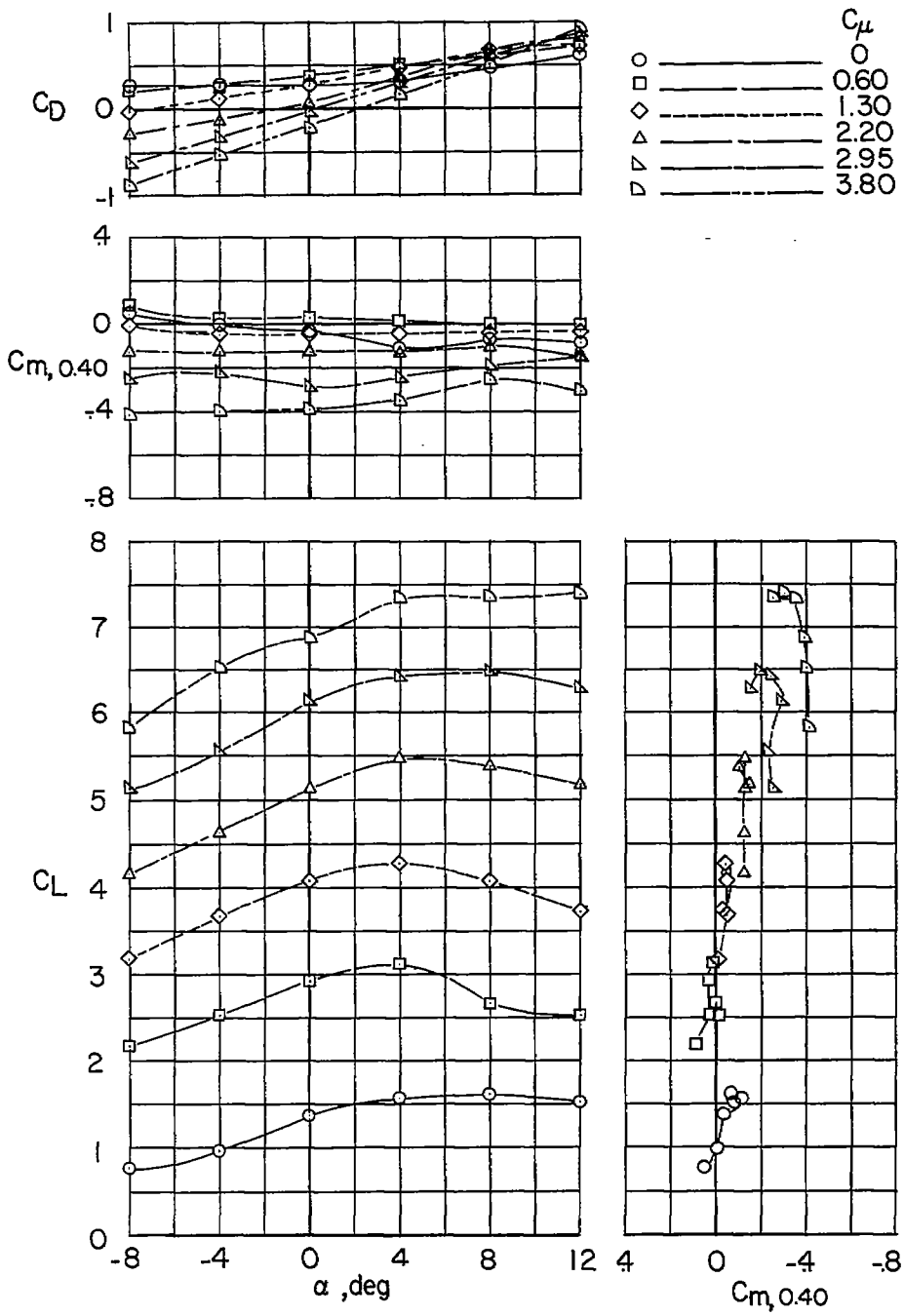

(b) $S_t/S = 0.17$; $i_t = 15°$.

Figure 16.- Continued.

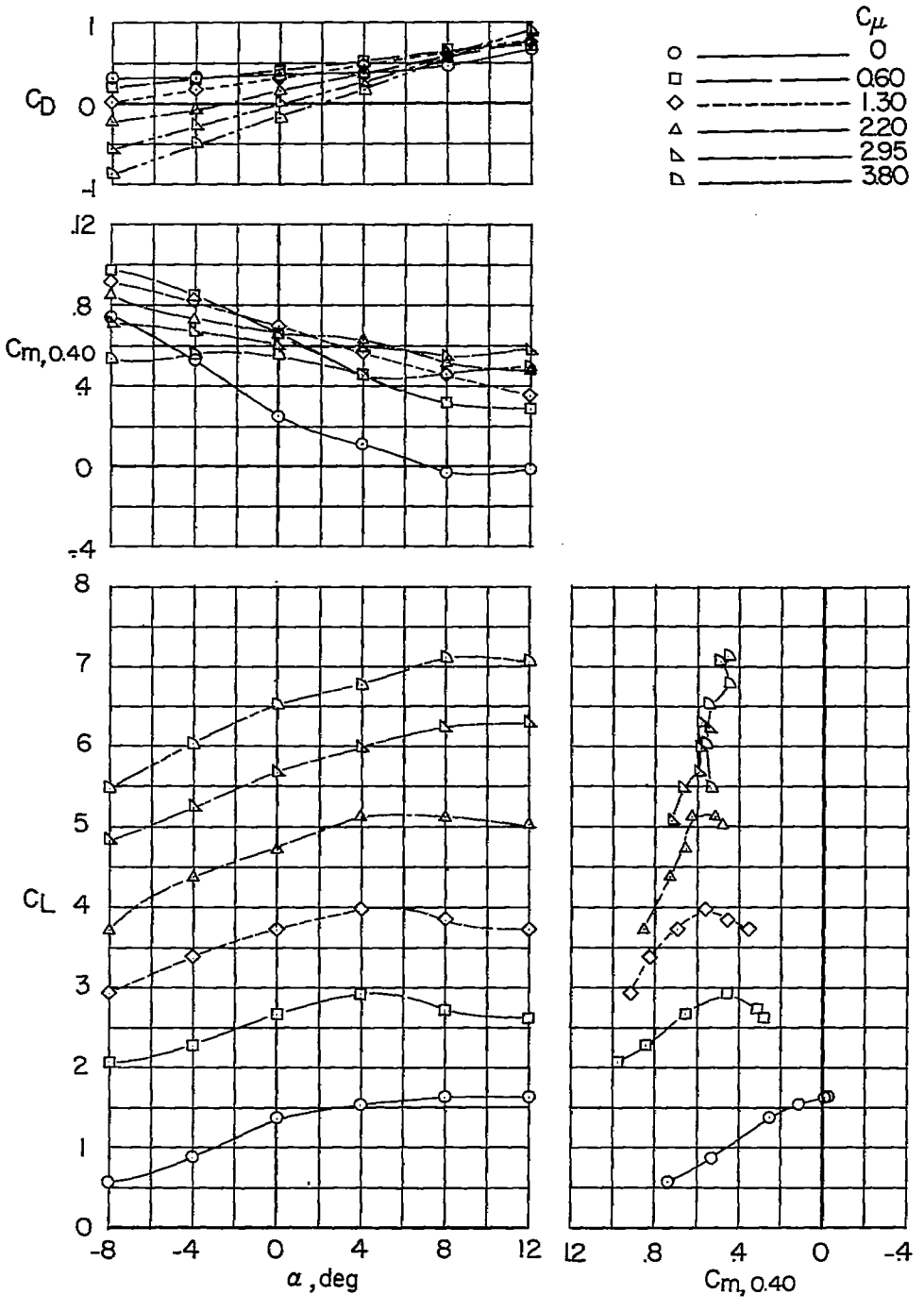

(c) $S_t/S = 0.34$; $i_t = 10^\circ$.

Figure 16.- Continued.

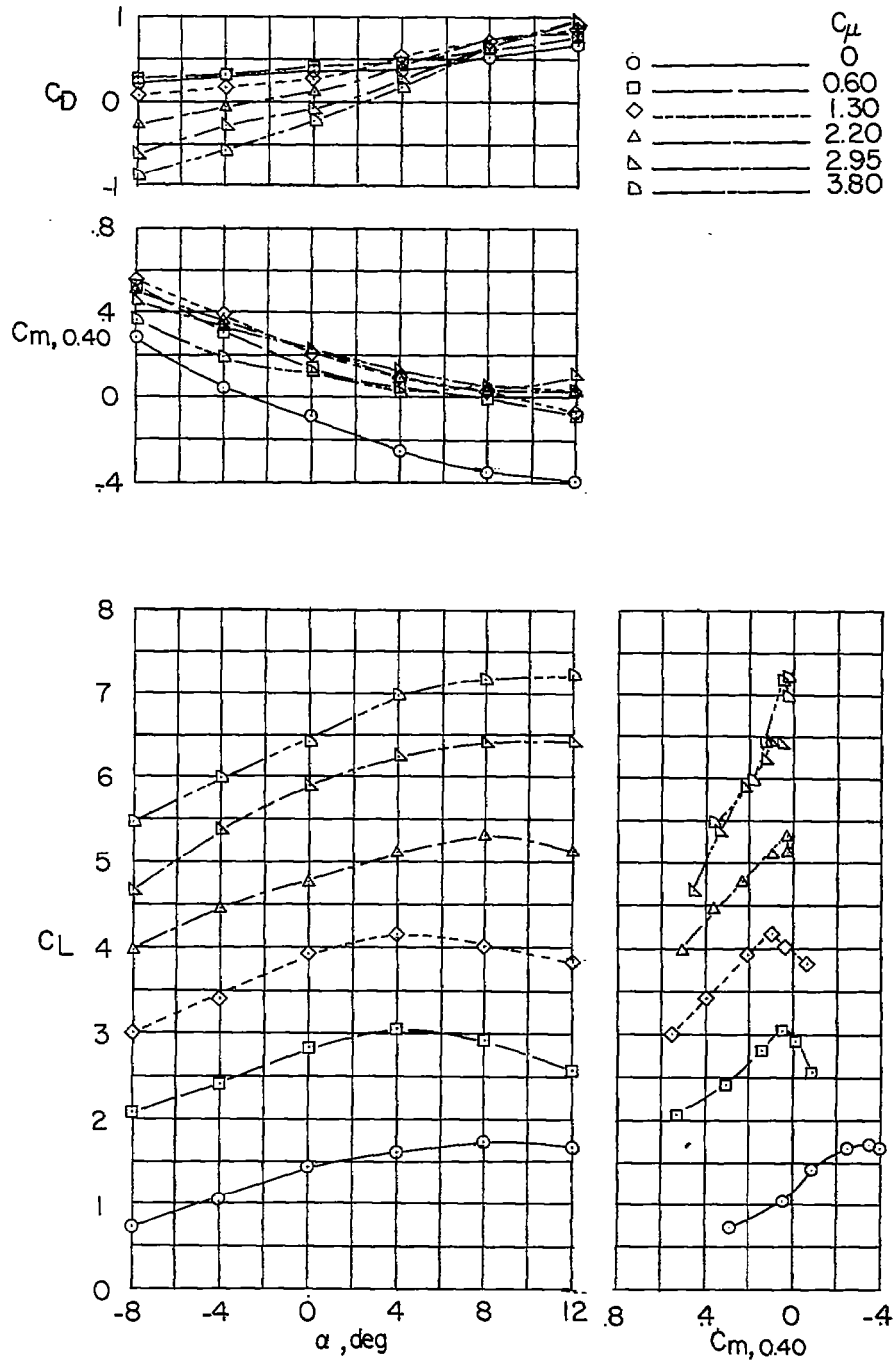

(d) $S_t/S = 0.34$; $i_t = 15°$.

Figure 16.- Concluded.

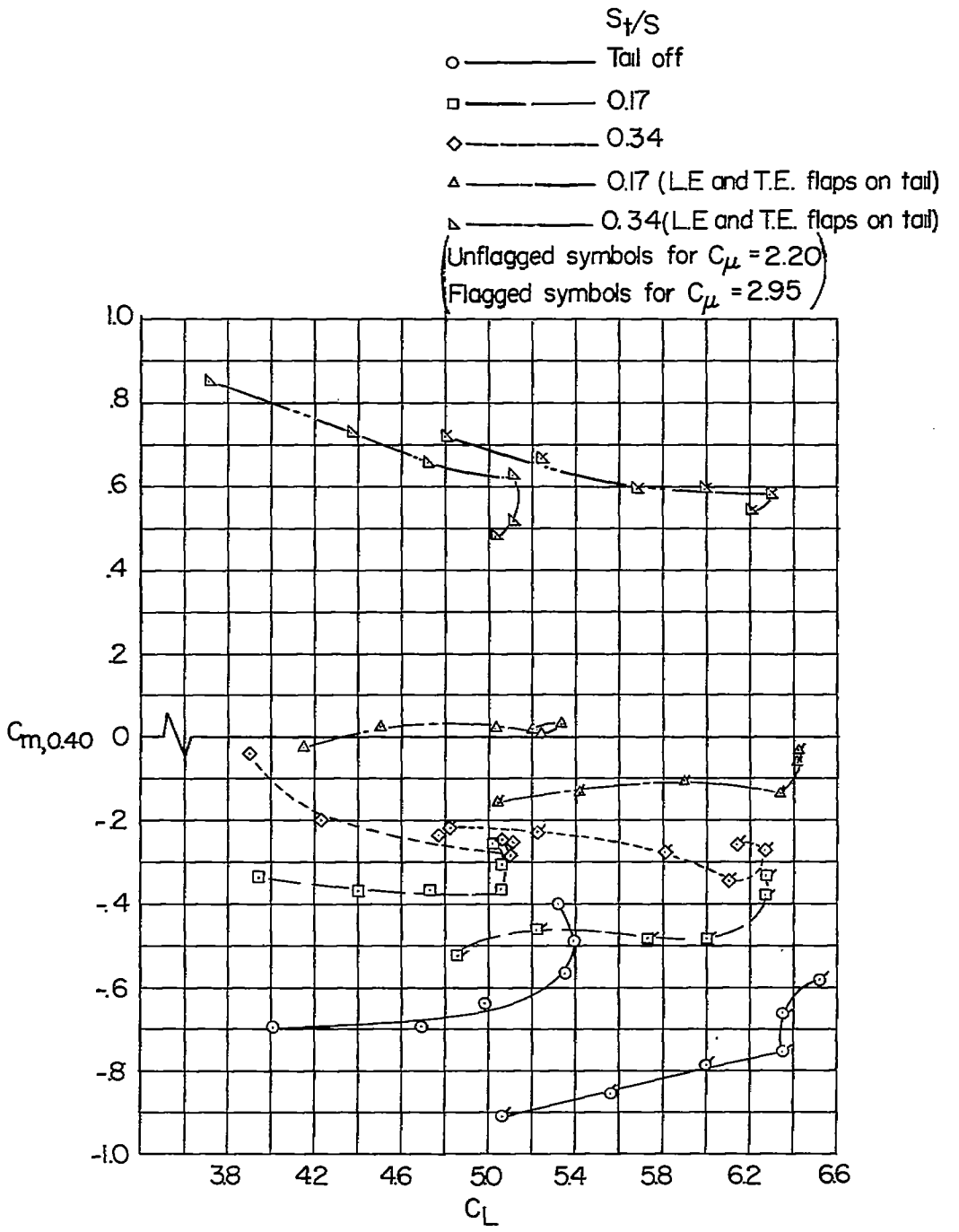

Figure 17.- Summary of pitching-moment data for various horizontal-tail configurations for values of C_μ of 2.2 and 2.95 for the high-wing two-jet swept-wing model. High-tail arrangement; $i_t = 10^\circ$; $\delta_f = 60^\circ$.

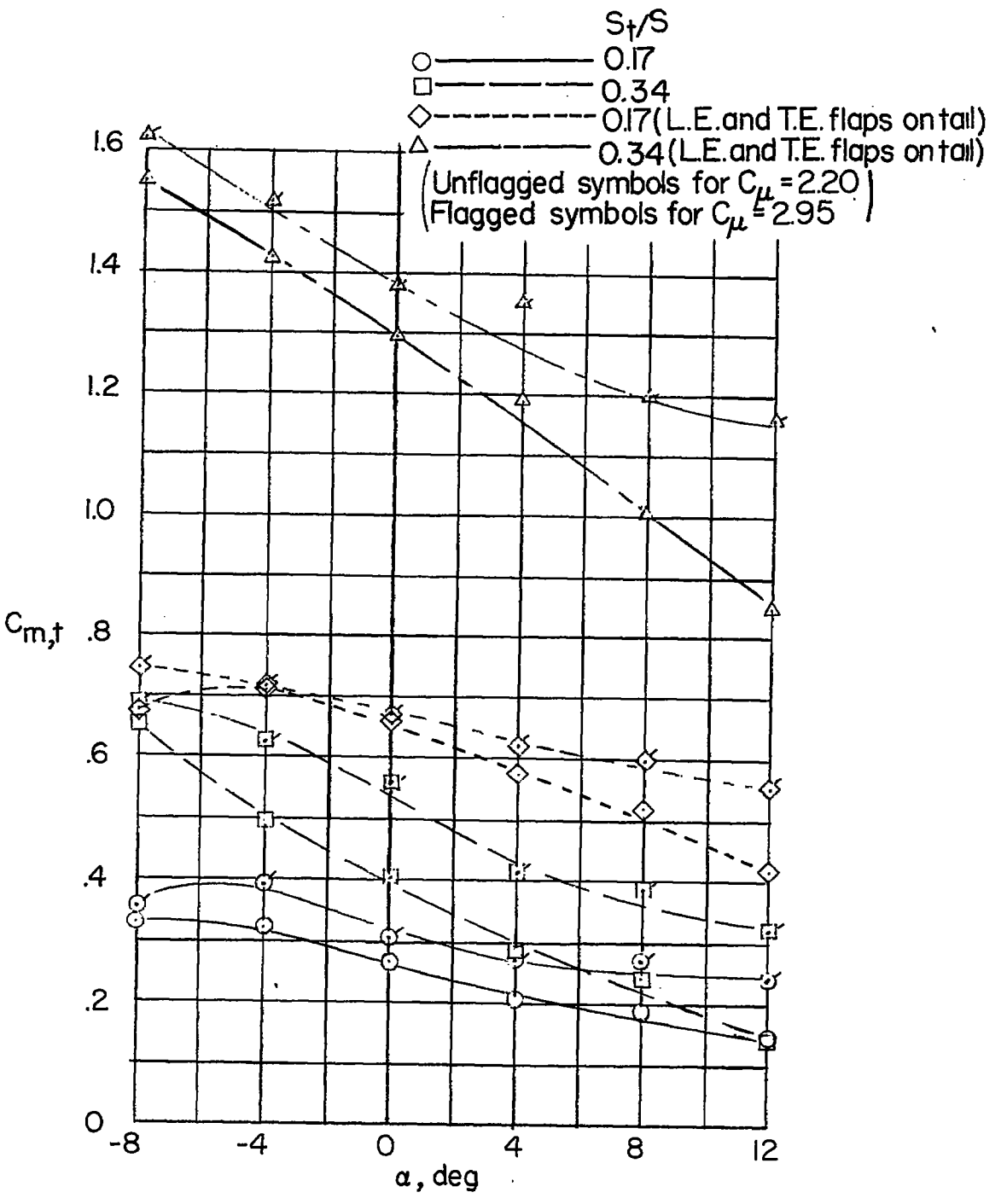

Figure 18.- Pitching-moment increments produced by various horizontal-tail configurations (data obtained from fig. 17). $i_t = 10^\circ$; $\delta_f = 60^\circ$.

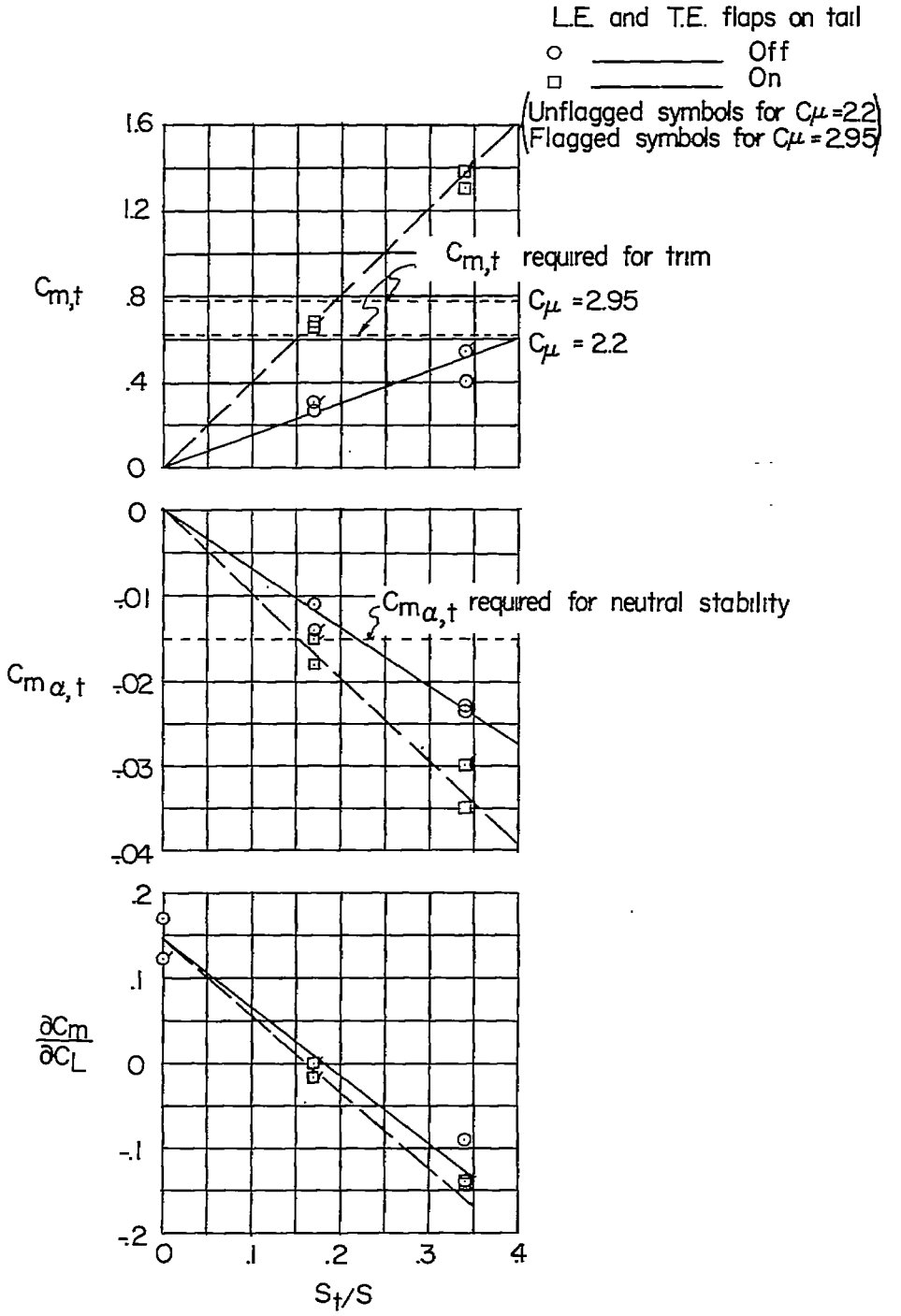

Figure 19.- Variation of longitudinal stability and trim parameters with horizontal-tail area (values obtained from figs. 17 and 18 at $\alpha = 0^{\circ}$).

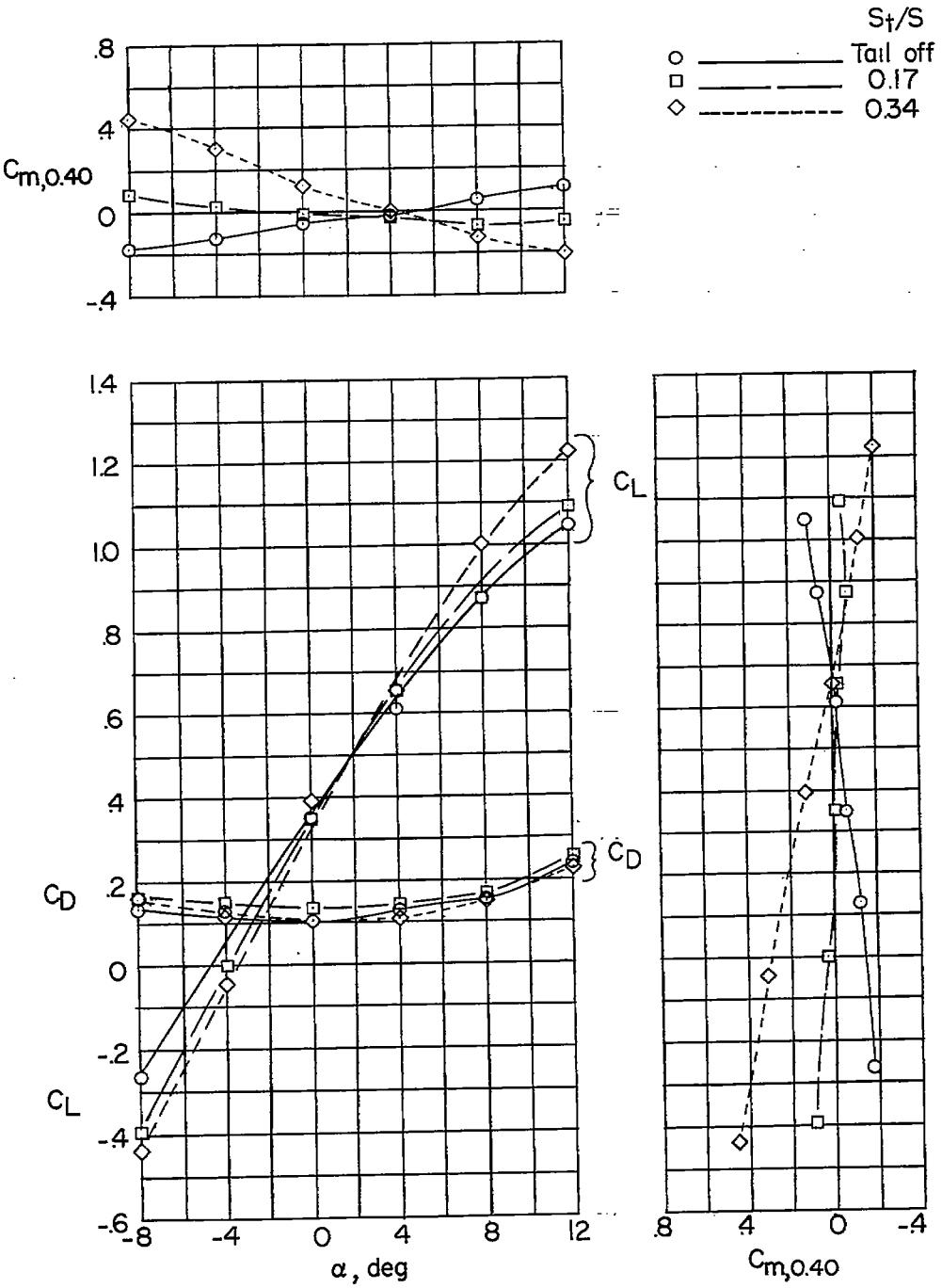

Figure 20.- Longitudinal stability characteristics of the high-wing two-jet swept-wing model in the cruise configuration (flap and deflectors retracted). $C_\mu = 0$.

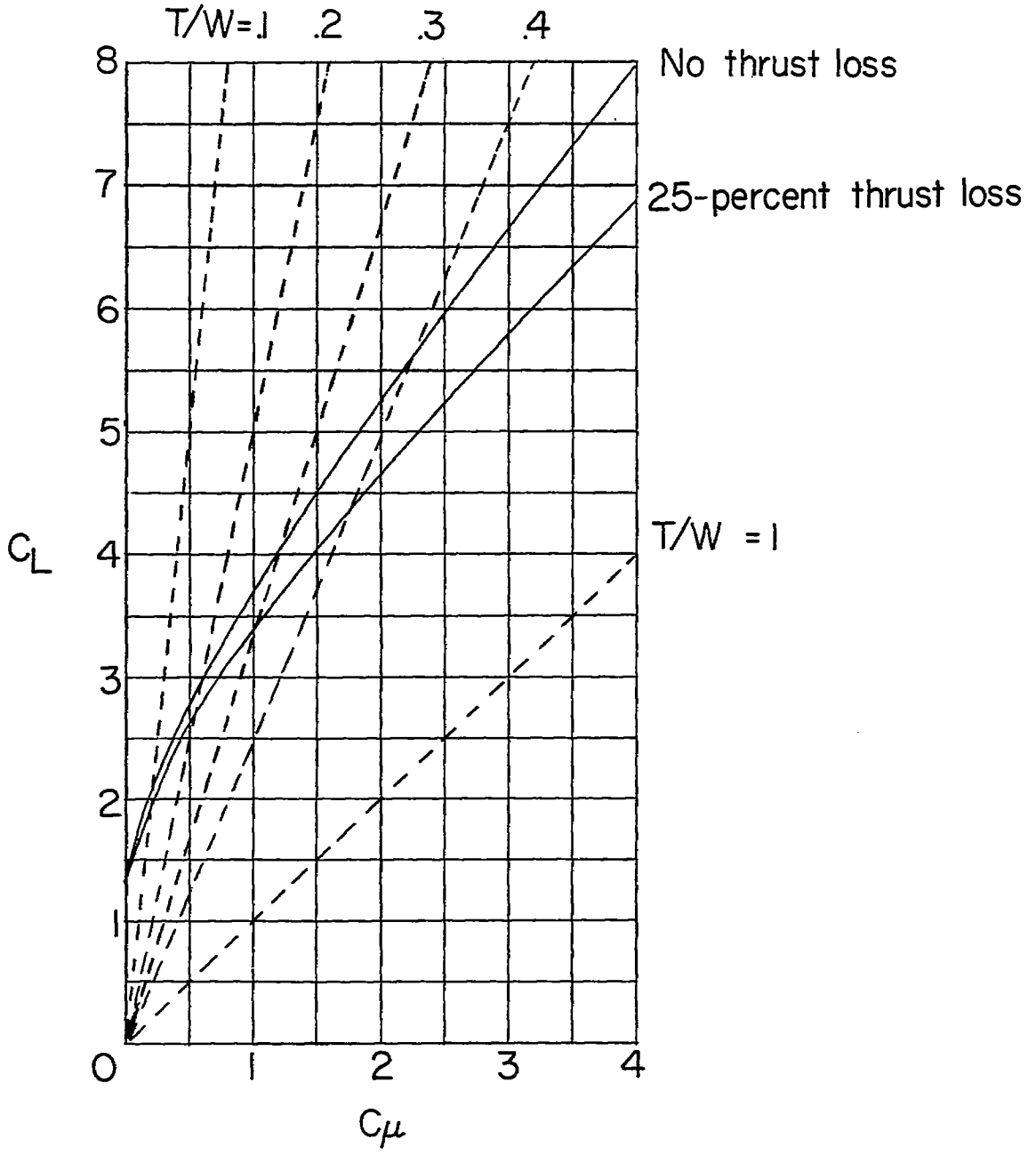

Figure 21.- Variation of lift coefficient with thrust coefficient for the high-wing two-jet swept-wing model. High-tail arrangement; leading- and trailing-edge flaps on the horizontal tail; $S_t/S = 0.17$; $\alpha = 0^\circ$.

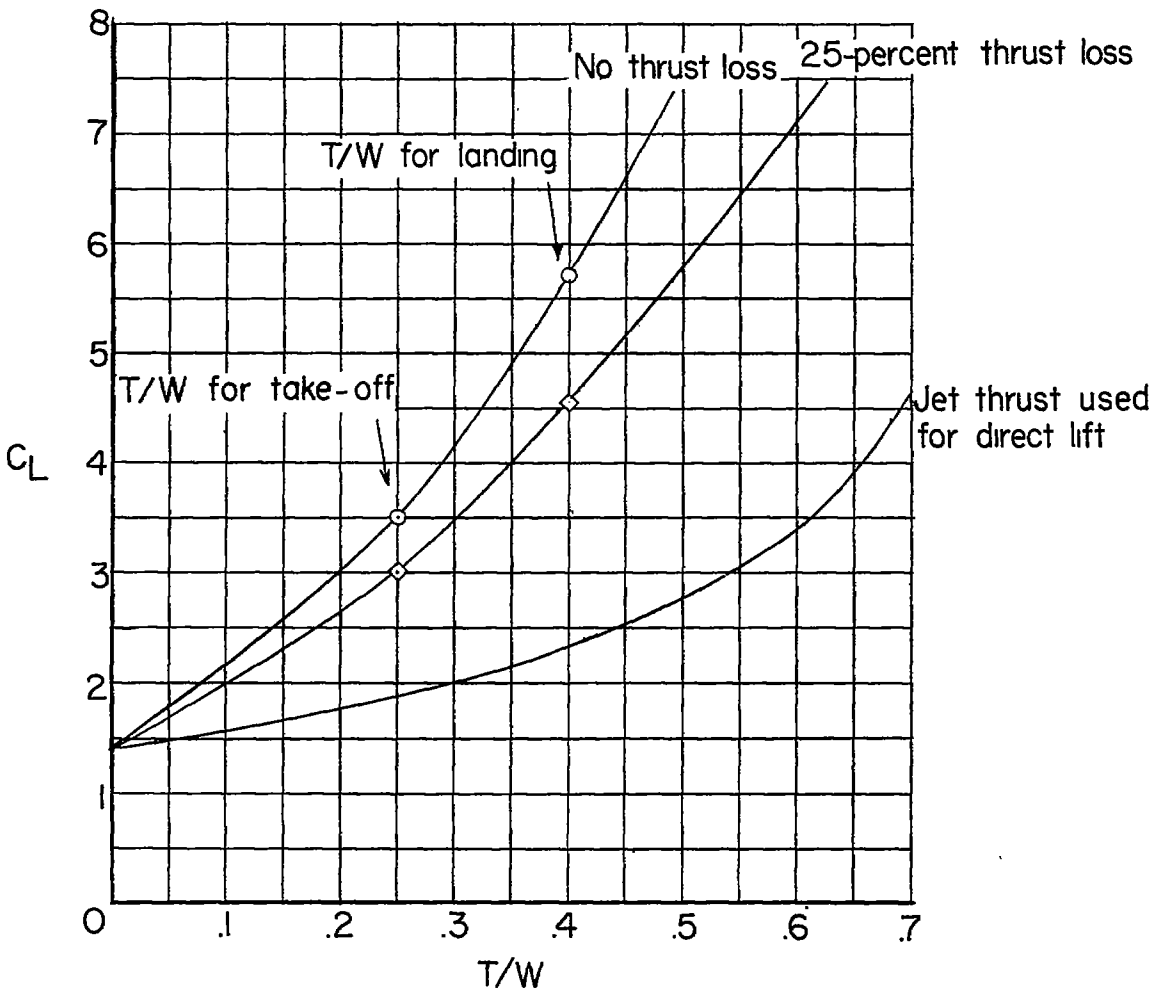

Figure 22.- Variation of lift coefficient with thrust-weight ratio for the high-wing two-jet swept-wing model (data obtained from fig. 21). High-tail arrangement; leading- and trailing-edge flaps on the horizontal tail; $S_t/S = 0.17$; $\alpha = 0^\circ$.

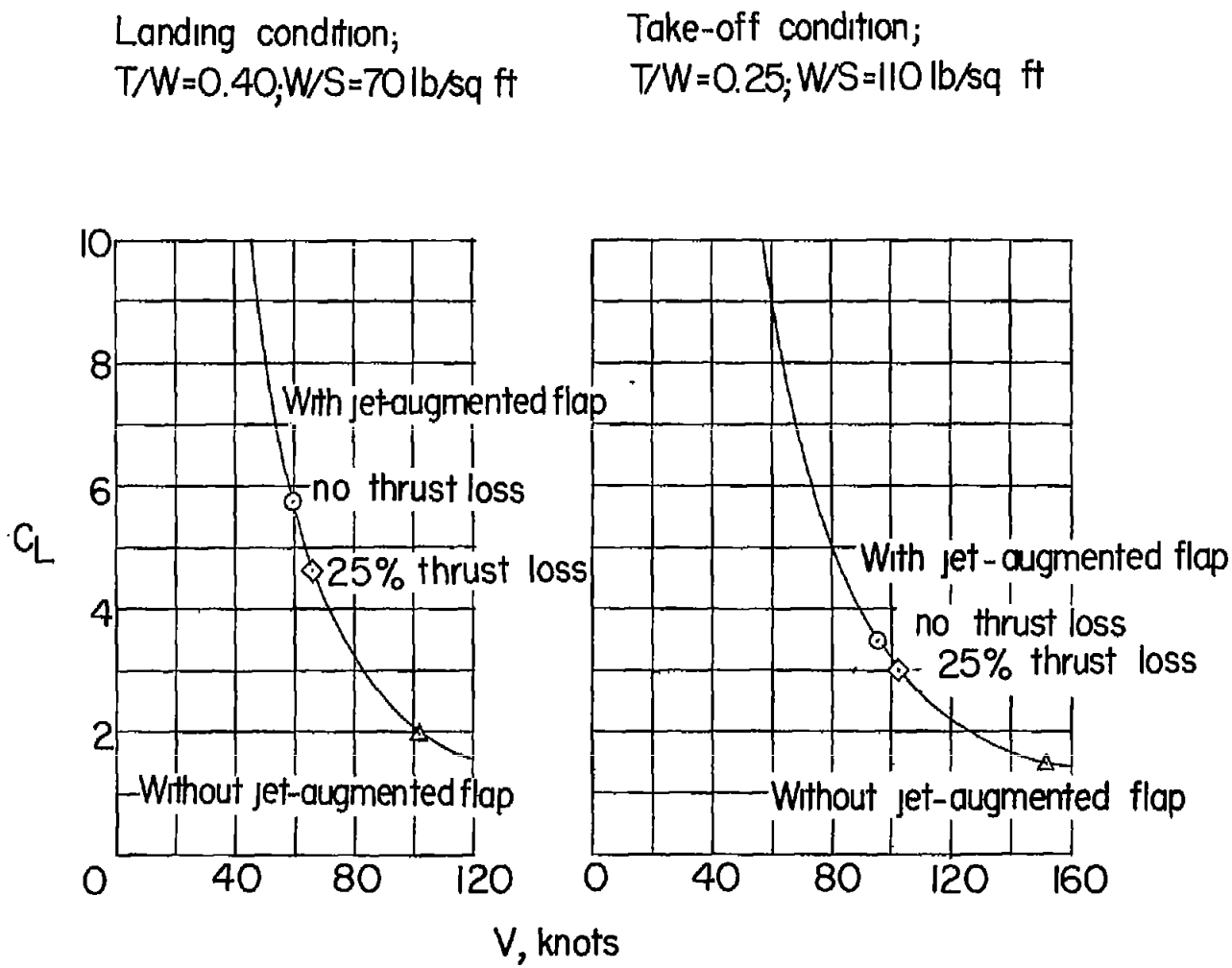

Figure 23.- Calculated minimum take-off and landing velocities for a jet transport or bomber airplane with an external-flow jet-augmented slotted flap (calculations based on lift data of fig. 22).